APTD-1088

PB 209 479

TRW REPORT NO.
14103-6004-R0-00

LASER HOLOGRAPHY STUDY OF OIL-FIRED BURNER COMBUSTION

Reproduced by
NATIONAL TECHNICAL
INFORMATION SERVICE
Springfield, Va. 22151

ENVIRONMENTAL PROTECTION AGENCY

61

This report was furnished to the Environmental Protection Agency by TRW Systems Group in fulfillment of Contract CPA 70-4, Modification 7. The contents of this report are reproduced herein as received from TRW Systems Group. The opinions, findings and conclusions expressed are those of the authors and not necessarily those of the Environmental Protection Agency. Mention of company or product names does not constitute endorsement by the Environmental Protection Agency.

300

BIBLIOGRAPHIC DATA SHEET	1. Report No. APTD-1088	2.	3. Recipient's Accession No.

4. Title and Subtitle
Laser Holography Study of Oil-Fired Burner Combustion

5. Report Date
November 1971

6.

7. Author(s)
A. B. Witte and B. J. Matthews

8. Performing Organization Rept. No. 14103-6004-RO-00

9. Performing Organization Name and Address
TRW Systems Group
One Space Park
Redondo Beach, California 90278

10. Project/Task/Work Unit No.

11. Contract/Grant No.
CPA 70-4

12. Sponsoring Organization Name and Address
ENVIRONMENTAL PROTECTION AGENCY
Technical Center
Research Triangle Park, North Carolina 27711

13. Type of Report & Period Covered

14.

15. Supplementary Notes

16. Abstracts The primary objective was to design instrumentation and evaluate its feasibility for characterizing flame turbulence and temperature gradient for several burner configurations. In this way, it may be possible to relate basic flame characteristics to the generation of emissions, particularly NO which is formed and fixed in the primary combustion zone. The feasibility of recording fog-free holographic interferagrams of residential fuel fired oil burner flames was demonstrated with two holocameras designed to observe the near and far field of the burner. The most important feature observed interferometrically was that the flame structure is extremely turbulent. This turbulence made it impossible to resolve the fringe pattern on the centerline of the burner. Preliminary data reduction of the interferograms showed that on the outside edge of the burner, the temperature gradient, $\frac{\Delta T}{\Delta R}$, was about 800 F/inch. Barewire thermocouple measurements made of the flame were corrected for radiation, and are believed to be lower than the true flame temperature because of fuel droplet impingement and evaporation. Excellent quality holographic interferograms were recorded of a small burner (Bernzomatic burner). Fringes could be resolved, read and interpreted. Temperature gradients calculated at the edge of this laminar flame were about a factor of 10 higher than for the Beckett fuel oil burner turbulent flame. Recording a holographic interferogram of a hot air gun showed the feasibility of controlling the turbulence level of a flame-like hot gas. Preliminary data were also reduced in this case.

17. Key Words and Document Analysis. 17a. Descriptors
Air pollution
Lasers
Oil burners
Combustion
Photographic recording
Turbulence
Temperature

17b. Identifiers/Open-Ended Terms

17c. COSATI Field/Group 13B

18. Availability Statement	19. Security Class (This Report)	21. No. of Pages
Unlimited	UNCLASSIFIED	61
	20. Security Class (This Page) UNCLASSIFIED	22. Price

LASER HOLOGRAPHY STUDY

OF

OIL-FIRED BURNER COMBUSTION

Prepared by

A. B. Witte and B. J. Matthews

TRW Systems Group

One Space Park

Redondo Beach, California 90278

Contract CPA 70-4

ENVIRONMENTAL PROTECTION AGENCY

Technical Center

Research Triangle Park, North Carolina

November 1971

FOREWORD

This report summarizes the holographic interferometry studies of oil fired burner flames accomplished under Environmental Protection Agency Contract CPA 70-4, Modification No. 7, dated 20 April 1971. This report is submitted by TRW Systems Group, TRW, Inc., in accordance with provisions of the modified contract.

Work on this contract was accomplished by personnel of the TRW Fluid Mechanics Laboratory. The Principal Investigator was Dr. Arvel B. Witte. Dr. Ralph F. Wuerker of TRW's Systems Group Research Staff served as a consultant in the areas of laser physics and holocamera design. The TRW Project Manager was Mr. Birch J. Matthews. Technical direction and administration of the contract for the Environmental Protection Agency was the responsibility of Messrs. William B. Kuykendal and Robert M. Statnick.

The authors wish to thank Messrs. Frank Gomes and Bruce Winston of the TRW Fluid Mechanics Laboratory for their assistance in conducting the holography experiments. In addition, the assistance and cooperation of Mr. Blair Martin of the Environmental Protection Agency was greatly appreciated.

CONTENTS

		Page
1.	INTRODUCTION	1
2.	EXPERIMENTAL APPARATUS	3
	2.1 FUEL OIL BURNERS	3
	2.2 LASER HOLOGRAPH DEVELOPMENT	3
	2.3 THERMOCOUPLE PROBES	11
3.	TEST PROCEDURE	15
4.	DATA REDUCTION PROCEDURE	17
5.	RESULTS	21
	5.1 SEQUENCE OF PROGRESS AND PROBLEMS SOLVED	21
	5.2 HOLOGRAMS	21
	5.3 HOLOGRAPHIC INTERFEROGRAMS	23
	5.4 INTERFEROGRAM DATA REDUCTION	35
	5.5 THERMOCOUPLE MEASUREMENTS	40
6.	CONCLUSIONS	44
7.	RECOMMENDATIONS	45
8.	REFERENCES	46
	APPENDIX A, THERMOCOUPLE RADIATION CORRECTION, CONDUCTION LOSSES AND FREQUENCY RESPONSE	

ILLUSTRATIONS

		Page
1.	ABC Standard Burner	3
2.	ABC Mite Burner	4
3.	Beckett Bantam Burner	5
4.	Burner Test Rig	6
5.	Schematic of Wide-Angle Two-Beam Transmission Holocamera	7
6.	Schematic of Holocamera Scene Volume, Maximum View Angel, and Fog-Reducing Shutter Position..	12
7.	Chromel-Alumel Flame Thermocouples	14
8.	Hologram of Coordinate Systems and Background Grid	22
9.	Burner Spray Pattern Burner Off. Spray on for 2 Seconds	24
10.	Burner Spray Pattern Burner Off. Spray on for 2 Seconds	24
11.	Reconstruction photographs of a ruby laser interferogram of open flame combustion from the ABC Mite oil burner. The photos differ by the focus of the copy camera. The direction of flow is from right to left.....	26
12.	Burner Interferogram. Burner on for 5 Seconds...	28
13.	Burner Interferogram. (Reconstructed from Bleached Plate). Burner on for 5 Seconds	28
14.	Burner Interferogram (Reconstructed from Bleached Plate). Burner on for 1 Second	29
15.	Infinite Fringe Interferogram of ABC Mite Burner Centered at 10 inches from Head	29
16.	Interferogram of ABC Mite Burner	30
17.	Infinite Fringe Interferogram Combustion Starting Transient in ABC Mite Showing Intermittent Combustion	32

1. INTRODUCTION

Furnace emission characterizations and fuel demand data for oil burners indicate that during winter months space heating is a significant source of SO_x, NO_x and particulate emissions. A recent evaluation of flame retention devices on small space heater, high pressure atomizing gun burners showed that these emissions can be substantially reduced.[1] However, it is not obvious why some of these retention devices are more effective than others, although the microstructure of the resulting flame is thought to influence emission levels.

The primary objective of this project was to design instrumentation and evaluate its feasibility for characterizing flame turbulence and temperature gradient for several burner configurations. In this way, it may be possible to relate basic flame characteristics to the generation of emissions, particularly NO which is formed and fixed in the primary combustion zone.

Previous work at TRW has shown laser holography to be an effective research tool in the study of high temperature phenomenon.[2,3] Laser holography offers an opportunity to permanently record for later detailed study high resolution flame detail in three dimensions. In addition, the resulting high energy, coherent illumination is sufficient to penetrate radiant flames while producing a high signal to noise ratio.

In all studies of this type, the main problem encountered is film fogging by a luminous subject. Temperature data have been calculated from holographic interferograms in former studies involving turbulent wakes.[4,5] The primary requirement imposed by the data reduction procedure upon the data is that fringes can be resolved, numbered, and that only small statistical excursions from an otherwise axisymmetric mean flow are encountered. This latter restriction can be removed when holocameras are developed with 180° viewing as is now believed to be possible.[6]

The following sections of this report describe the experiments and discuss the experimental technique (Sections 2 and 3, respectively). Data from the experimental program is analyzed in Section 4. The results are summarized in Section 5.

2. EXPERIMENTAL APPARATUS

2.1 FUEL OIL BURNERS

A schematic of each high-pressure atomizing-gun burner is shown in Figures 1, 2, and 3. The fuel oil was No. 2 distillate obtained from Gulf crude. The oil had an API gravity equal to 36.* The fuel oil was gravity fed to the burner which was mounted in a test rig. A burner box 9 inches square by 15 inches in length with Pyrex No. 7740 glass sides was used to approximate actual operation while permitting optical access for holography. The flue gases were vented to the roof of the laboratory through a 20 foot stove pipe with the aid of a small exhaust fan. A schematic of the test rig is shown in Figure 4. Fuel comsumption of the ABC Mite was measured to be 1 ml/sec or about 0.9 gal/hr.

2.2 LASER HOLOGRAPH DEVELOPMENT

A significant fraction of the project effort was devoted to developing a laser holocamera suitable for producing high quality interferograms. This camera and the procedure for its application are described below.

Basic Laser Holograph - Short Scene Depth

The laser holograph is comprised of a puised ruby laser and a holocamera. The pulsed ruby is used in this investigation because sufficient energy can be produced to penetrate the burner flame during a pulse width small enough to stop the action of the combustion phenomena. The pulsed ruby laser has been described in detail in an earlier TRW report to EPA and will not be discussed further here.[7] The holocamera design is a modified version of the apparatus shown in Figure 5 developed on another contract[8] by Dr. Ralph Wuerker of TRW. Modifications to the holocamera shown in Figure 5 for use with this contract were as follows: (1) the angle described by mirror No. 5, the hologram and the quadruple lens set is 90° not 75°; (2) the scene beam-hologram angle is 45° not 52-1/2°; and, (3) a plate rotator was installed to permit finite fringe operation. The purpose of recording finite fringes is to avoid fringe ambiquity problems.

The advantages of this holocamera are that it has a very wide viewing angle (measured to be 40°)[9] and good resolution (about 20 microns).[10] The scene depth, namely the distance between the hologram and the objective lens is 17 inches. The side wall of the 9 x 9 inch square cross-section burner box was located about two inches from the quadratic lens set. This position permitted the largest viewing aperture of the burner box; however, the aperture was not large enough to permit viewing of both top and bottom walls of the burner, a requirement imposed so that boundary conditions are known for data reduction purposes. The scene depth was subsequently expanded so that the burner side wall could be observed. A description of the larger scene depth holocamera follows.

---

* An API gravity of 36 is equivalent to a specific gravity of 0.845.

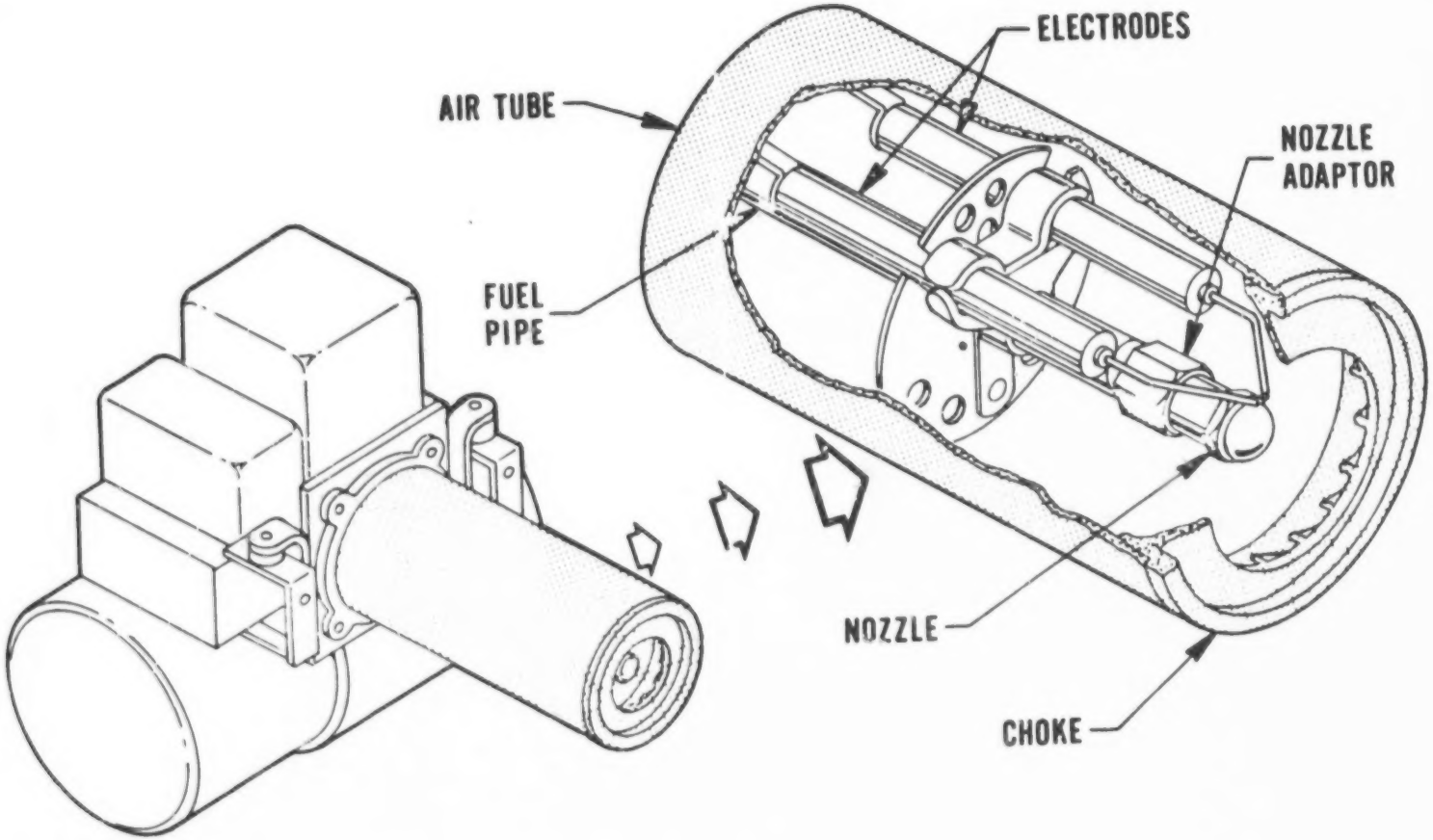

Figure 1. ABC Standard Burner.

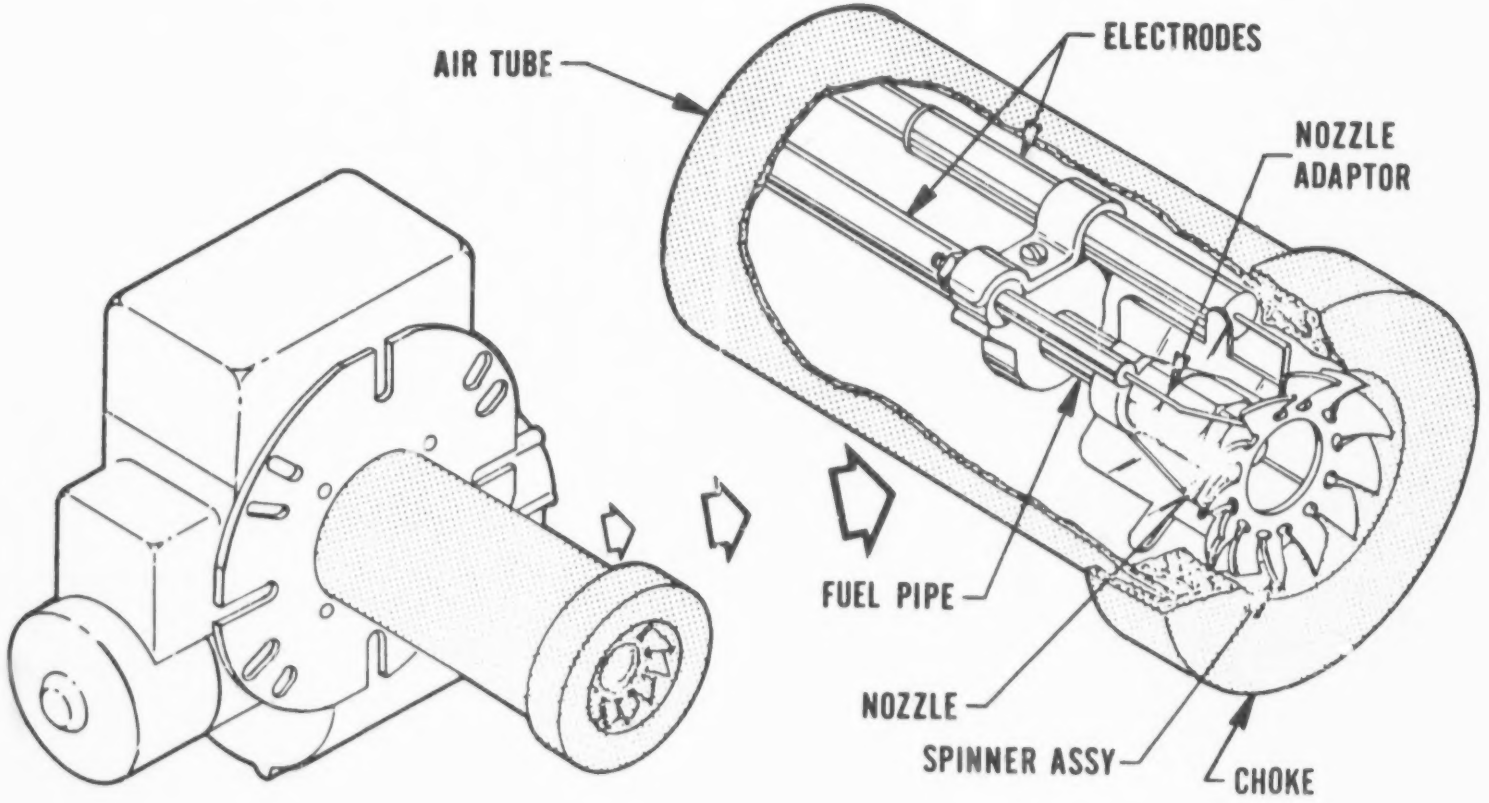

Figure 2. ABC MITE Burner.

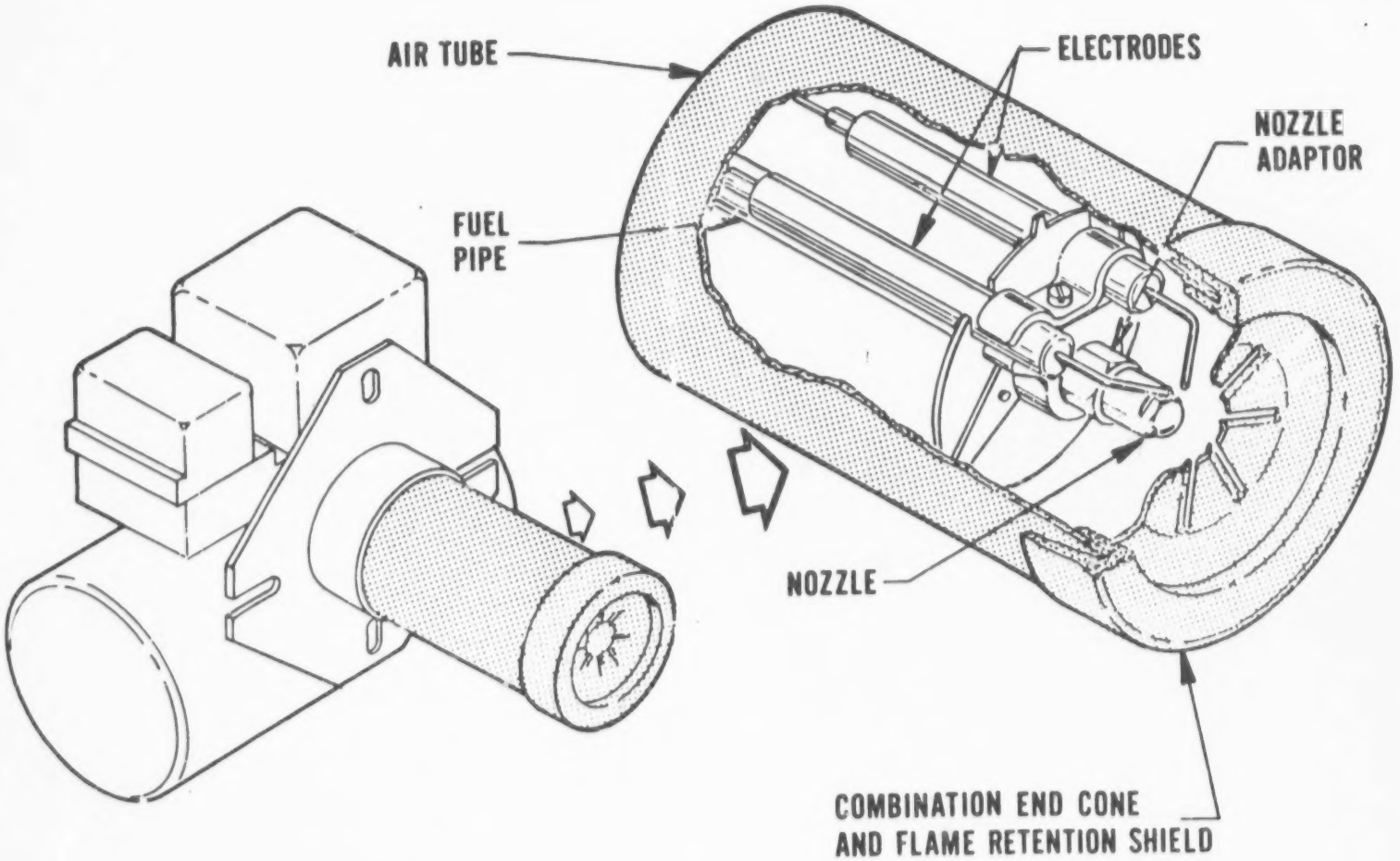

Figure 3. Beckett Bantam Burner.

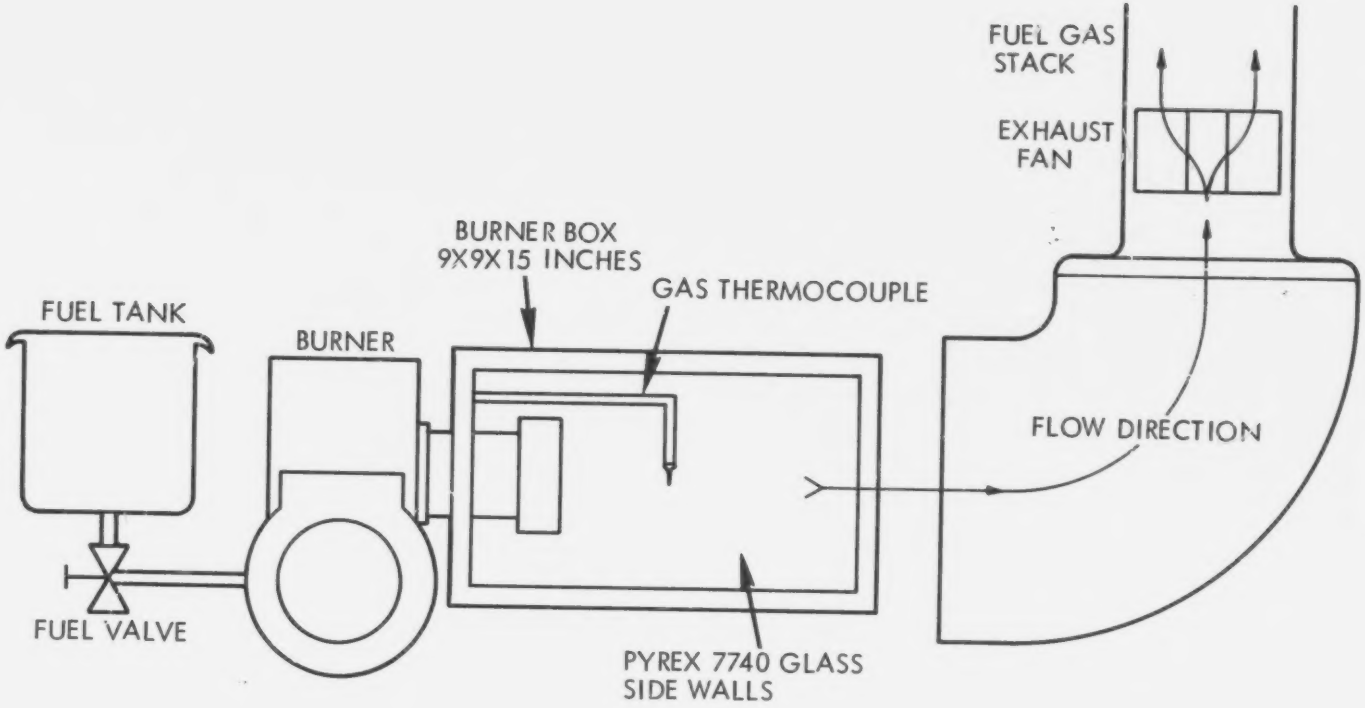

Figure 4. Schematic of Burner Test Rig.

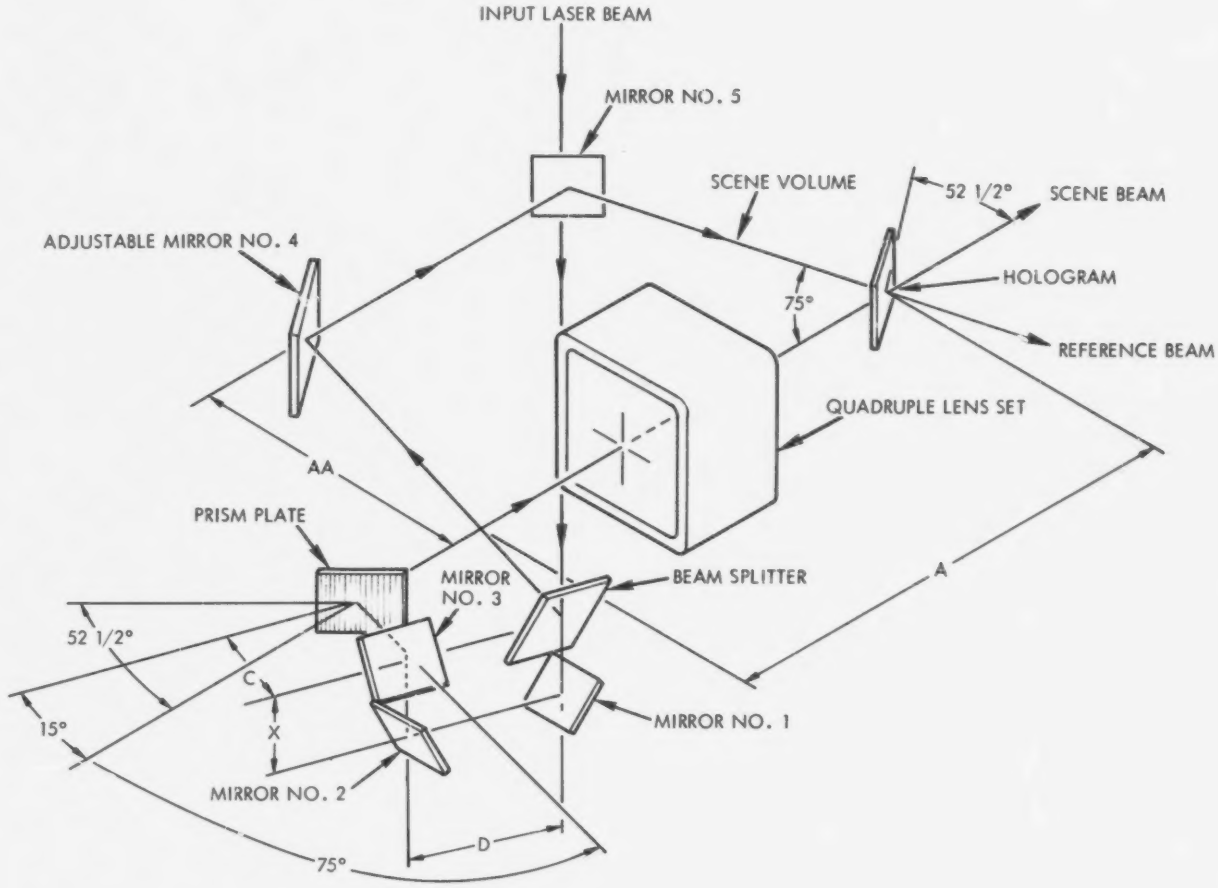

Figure 5. Schematic of Wide-Angle Two-Beam Transmission Holocamera.

Modified Laser Holograph - Large Scene Depth

One of the convenient features of the original 11 inch focal length objective lens set used in this holocamera is that the lens set was quadratic; namely, it had two matched pairs of glass lenses. (The quadratic set weighed 85 pounds).

Two iterations on holocamera design were implemented to extend the scene depth by about a factor of two. The first design utilized the two outer lenses of the quadruple lens set. This set comprised a concave-convex pair with a resultant focal length of 18 inches. Holograms recorded with this setup showed severe distortion. The inner lens set (focal length 20.5 inches), also a concave-convex pair, was next installed and proved to be superior in performance to the first set. Good quality holograms of a coordinate system in the scene volume as well as on the objective lens were recorded in the process of path matching the system. These modifications required that the holocamera be lengthened by a factor of two. Modifications were accomplished by the addition of sections to each end of the "breadboard" holocamera. The new system allows observation of the top and bottom of the box.

Helium Cell Fringe Compensator Design

The purpose of the compensator is to reduce the overall fringe shift so that it will remain within the picture (hologram). This apparatus will not reduce the sensitivity of the index of refraction changes and gradients (density, temperature gradients). The compensator is comprised of a plexiglass box 6 inches deep with a 13 inch square cross-section. During the comparison beam exposure, the compensator (box) is filled with helium at atmospheric pressure. During scene beam exposure, the box is filled with air at 1 atmosphere. The compensator was bolted to the quadratic lens set mount on the side opposite the hologram plate.

If the box filled with air comprises the comparison scene, denoted subscript 2, and the box filled with helium comprises the test scene, denoted subscript 1, then the fringe shift relation is developed.

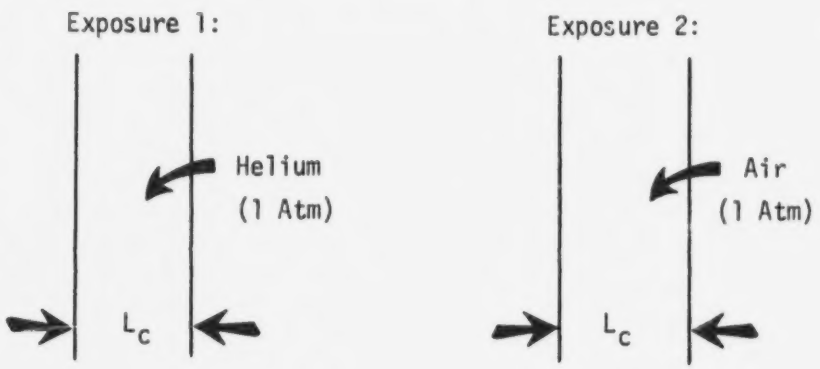

For the case of planar geometry the fringe number becomes:

$$S = \frac{1}{\lambda} (n_1 - n_2) L_c$$

where the index of refraction

$$n_i = 1 + \beta_i \frac{\rho_i}{\rho_{si}}$$

After some algebra, one obtains

$$S = \frac{1}{\lambda} \beta_2 \frac{\rho_2}{\rho_{s2}} \left(\frac{P_1}{P_2} \cdot \frac{T_1}{T_2} \frac{\beta_1}{\beta_2} - 1 \right) L_c$$

where

S = fringe shift

β_i = Gladestone-Dale constant for species i (2.92×10^{-4} for air and 0.36×10^{-4} for helium)

ρ = gas density

P = gas pressure

T = temperature

λ = radiation wavelength

L_c = cell width (15cm)

and subscript

s = standard conditions of temperature and pressure at which both β's are evaluated.

Taking $P_1 = P_2$, $T_1 = T_2$, the result becomes

$$S = -3.32 L_c$$

$$= -50 \text{ fringes}$$

Thus, relative to air, helium causes a fringe shift of -50 fringes.

If the burner box were completely filled with 2000°F air, and

$$s = 4.2 \left(\frac{T_s}{T} - 1 \right) L_B,$$

then $S \simeq -74$ fringes (relative to air) where the burner box width $L_B = 22.5$ cm. Because the gas in the box is cooler at the walls, the absolute fringe shifts would be somewhat less. For the simplified case cited above, the fringe shift of the flame relative to helium would be about -24 fringes. Thus, the compensator so designed would appear to be adequate.

Shutters and Filters

In order to minimize film (plate) fogging it was necessary to experiment with a number of mechanical shutters to "shield" the film from the intense burner flame. Three shutters were evaluated.

Focal Plane Roller Blind Shutter --

This shutter had a 4 x 5 inch rectangular format and was of Graflex origin. In order to keep the dark (cloth) blind from burning, a large solenoid driven leaf type outer shutter, made by Harvard, was used to protect the blind. The fastest shutter speeds ranged between 80 and 100 milliseconds. Adverse fogging occurred at these speeds. The shutter was located at plane A-A in Figure 6.

Leaf Shutter 2-5/16 inch Diameter --

A spring-loaded shutter taken from a Fairchild camera was operated at 6 milliseconds, which removed the fogging problem but reduced viewing area. Solenoid actuation was added to the shutter. The shutter was located at position B-A in Figure 6.

Leaf Shutter 3-1/2 inch Diameter --

A spring-loaded shutter taken from a Kodak Air Force mapping camera was operated at 9, 18, and 40 milliseconds. At a shutter speed of 9 milliseconds, holograms and interferograms were essentially free of fog. In addition, this shutter has 3 times the area of the former shutter and thus allows substantially larger viewing angle of the flame. The shutter was located at position B-A in Figure 6.

Filters

Filters were used in order to reduce the amount of fogging during hologram plate exposure and thus increase the signal-to-noise ratio. The burner radiates strongly in the visible and infrared. A Kodak Wratten No. 70 filter was used to reduce the fogging by visible radiation. The transmission properties of the Wratten 70 filter are as follows:

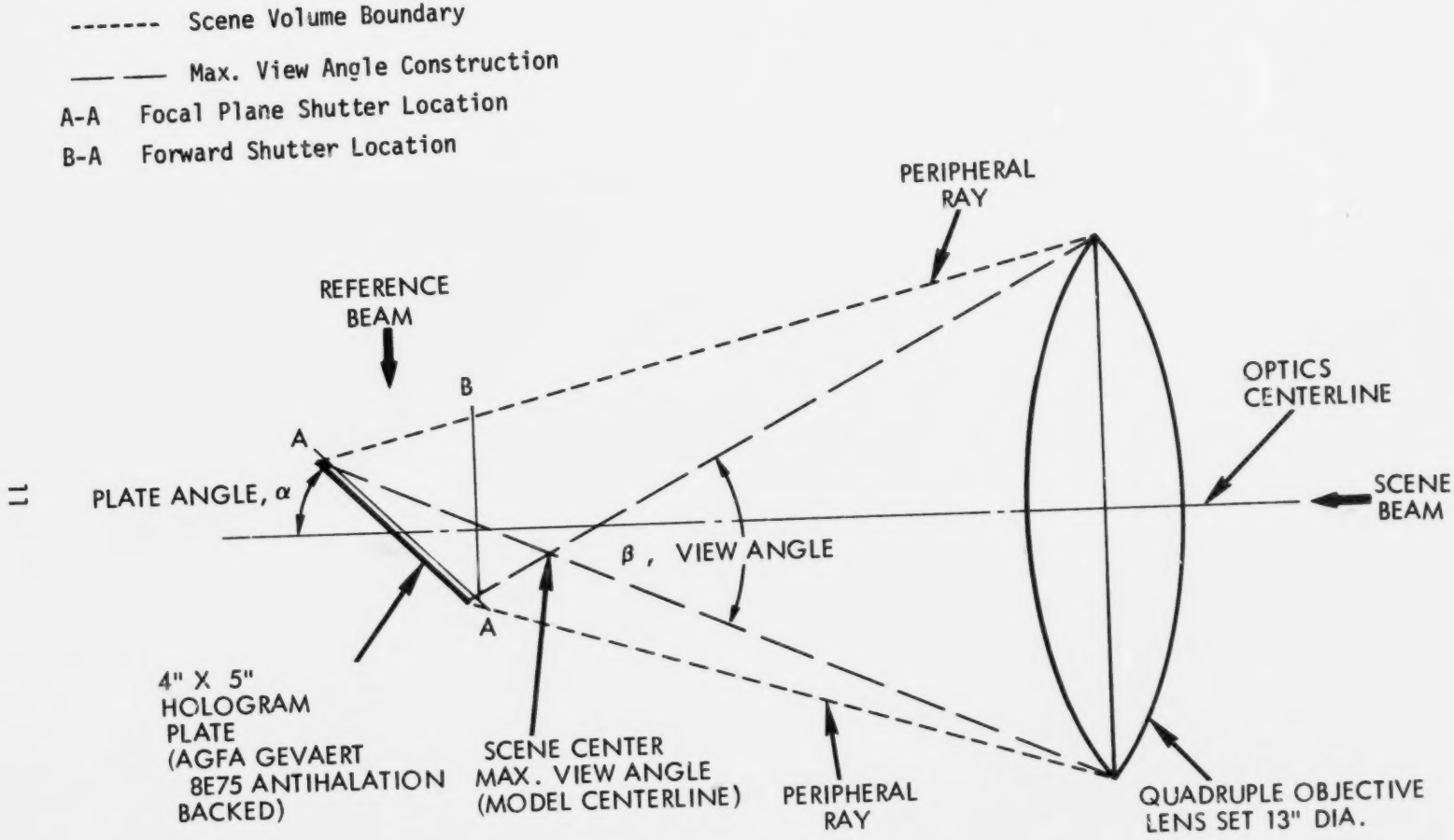

Figure 6. Schematic of Holocamera Scene Volume, Maximum View Angel, and Fog-Reducing Shutter Position

Wavelength in Microns (μ)	Percent Transmittance
.65	.63
.66	10.5
.67	35.0
.68	55.2
.69	70.3
.70	79.0

Good transmission properties are observed for wavelengths above 0.66μ with a transmittance of almost 79 percent at the ruby wavelength, λ = 0.6943μ. There are no good filters in the range of 0.7 and beyond (infrared) which do not exclude the ruby wavelength; however, the spectral response of Agfa 8E75 emulsion beyond 0.76μ is negligible. From the fog levels encountered early in the test program with the relatively slow speed focal plane shutter, one may conclude that these oil-fired burners radiate strongly in the 0.65 to 0.75μ region.

In addition to the Wratten No. 70 gelatin filter, Corning Glass Works filters number CS-2-58 and CS-2-64 were evaluated. These filters essentially duplicate the Wratten No. 70 in the visible, but also exclude radiation for λ>2.75μ. No difference in fog level was noted when the Corning glass filters were used in series with the Wratten No. 70 filter.

2.3 THERMOCOUPLE PROBES

Probe Design

Both shielded and unshielded chromel-alumel thermocouple probes were built during the program. It was desired to measure both mean temperature and temperature fluctuation. Installation of the probes in the burner box was accomplished using a swivel-seal joint located near the head end of the burner box. The swivel joint permitted temperature traverses to be made during burner operation.

The mean temperature measurement thermocouples were packed in a refractory oxide insulation surrounded by an inconel sheath. The junction was formed by stripping back the inconel sheath. Probe construction is shown in Figure 7. The unshielded junction mean temperature probe (Figure 7a) used 0.051 inch diameter wires to demonstrate that chromel-alumel thermocouples could be used in the burner combustion environment.

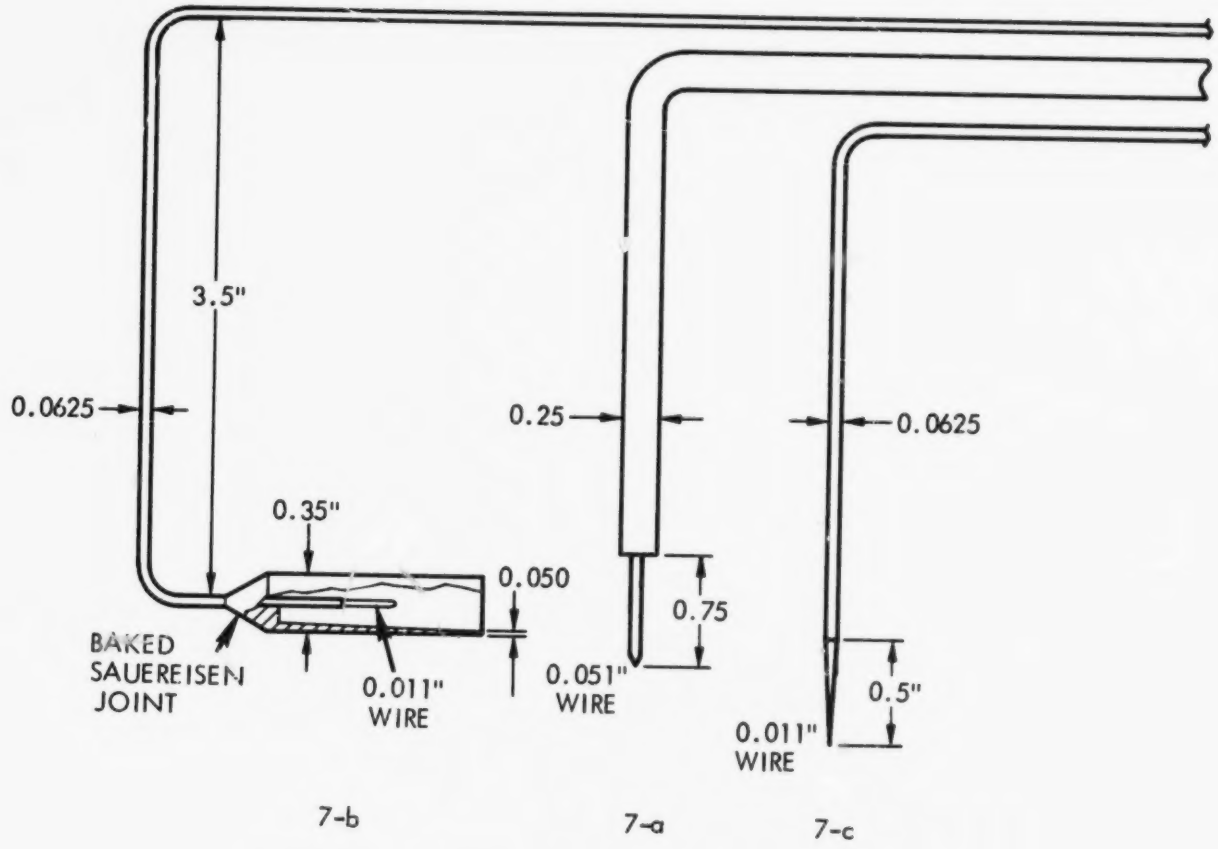

Figure 7. Chromel-Alumel Flame Thermocouples

Radiation losses occur when unshielded thermocouples are employed in a high temperature environment. Recognizing that a radiation shield would be needed to minimize these losses, the probe shown in Figure 7b was designed and built. The thermocouple junction now exchanges radiation with the hot refractory shield rather than the "cold" walls of the burner box. Holes were drilled in the shield to allow the hot gases to aspirate over the thermocouple junction. In this design, smaller wires (0.011 inch diameter) were chosen to minimize the conduction losses to the support.

The thermocouple probe designed to measure temperature fluctuations is shown in Figure 7c. Use of a radiation shield would seriously impair the time response of this type of probe. Thus, a correction must be applied to the measurement for radiation losses. Because of the large L/D of the wire, conduction losses to the support are negligible.

An estimate of unshielded thermocouple error due to radiation losses and an analysis of thermocouple frequency response to the turbulence of the flame is presented in Appendix A. In addition, conduction losses through the thermocouple support are also considered in the appendix.

3. TEST PROCEDURE

The test procedure was established and followed for recording holograms and interferograms of burner combustion. Starting with the burner in place, the following steps were taken to make the recordings:

1. Shutter cocked and energized
2. Room lights out
3. Uncover film plate
4. Record the comparison scene holographically
5. Recock shutter
6. Turn burner on
7. Record the test scene holographically
8. Turn burner off
9. Cover film plate
10. Lights on
11. Develop plate
12. Remove and clean windows on burner box.

In one instance, it was determined that the pyrex windows could only withstand about 90 seconds of uncooled operation before cracking. *

Not all of the flame interferometry recordings were made using the windowed burner box. Some recordings were taken with the box removed and the flame unconfined (open flame tests). For these tests, a piece of 1/4 inch thick Plexiglass plate was used to protect the quadruple lens set of the holocamera from flame impingement.

Some preliminary work was done with the helium cell; however, on the first formal test with this device, a slight overpressure resulted causing one of the Plexiglas wall bonds to fail. The cell was not used again during this program due to a reordering of priorities.**

---

* Use of a nitrogen gas purge over the windows would increase the operational life of the Pyrex windows. (In the future, quartz windows may have to be used if true adiabatic wall operating conditions seem desirable.

** Damage to the cell is minor and may be easily repaired such that the concept may be tried again in the future.

All of the interferograms and holograms were recorded on Agfa 8E75 anti-halation backed 4 x 5 inch glass plates.* Development time in Eastman Kodak HRP developer was typically 4 minutes for an interferogram. The acid fixer used was Nacco fix.

Interferograms were reconstructed with a Model 124A Spectra Physics helium neon gas laser ($\lambda = 0.6328\mu$) illuminator. The recordings were photographed using Polaroid Type 52 film having an ASA rating = 400. When desired, negatives of the reconstructed scene were made using Polaroid Type 55 P/N film.

---

* Product of Agfa-Gevaert, Antwerp, Belgium.

4. DATA REDUCTION PROCEDURE

Data reduction is comprised of three parts: photographing the desired view of the holographic interferogram and recording the fringe pattern using a microdensitometer; interpreting fringe number from the mincrodensitometer trace; and computing density by means of the standard equation for fringe shift,

$$S(x,y) = \frac{K}{\lambda} \int_0^z \left[\rho(x, y, z) - \rho_\infty\right] dz$$

The holographic interferogram is mounted in a reconstruction jig whose orientation is the same with respect to the reference beam as it was during the original recording of the holographic interferogram. During reconstruction, a 15 mw continuous wave He-Ne laser (λ = 0.6328 microns) was used to illuminate the holographic interferogram. A copy camera was positioned behind the holographic interferogram. The camera could be focused on the event which was a known distance behind the holographic interferogram and bounded by the viewing cone of the hologram.

The interferograms were photographed with either Polaroid Type 55 PN film which provides a positive and negative copy of the event using a nominal 1 to 10 second exposure at f/5.6 or Polaroid Type 52 which is about 8 times faster. The photographic density of the fringe pattern on these negatives was then recorded on a Joyce precision micro-densitometer having a slit size of about 0.010 inch by 0.010 inch.

Fringe number S was measured relative to the undisturbed (light fringe) background gas, i.e., relative to $S_\infty = 0$. The first dark fringe occurs where the change in optical path is $\lambda/2$. Interpretation of the change in optical path in wavelengths of light, i.e., fringe number S, is aided by keeping in mind the standard equation for fringe shift. Starting at the edge of the flame the fringe number begins to decrease, the first dark fringe yielding a value of S = 1/2 fringe.

The mean density profile calculations carried out here were made under the assumption that the flow field was axisymmetric. With the assumption of axisymmetric flow, the equation can be inverted as the Abel integral to obtain[12]

$$\rho(y) - \rho_\infty = -\frac{\lambda}{\pi K} \int_{y^2}^{r_s^2} \frac{\frac{ds}{dr^2}\, dr^2}{(r^2 - y^2)^{1/2}}$$

When this equation is rewritten as

$$\rho(y) - \rho_\infty = -\frac{\lambda}{\pi K} 2 \int_{y^2}^{r_s^2} \frac{ds}{dr^2} \, d(r^2 - y^2)^{1/2}$$

it may be cast into the following finite difference form (the Schardin-van Voorhis approximation[13]) for which the density is assumed constant in each of N thin angular rings of thickness Δ:

$$\rho(y) - \rho_\infty =$$

$$\frac{2\lambda}{\pi \Delta K} \sum_{k=i}^{N-1} (S_k - S_{k+1}) \frac{\sqrt{(k+1)^2 + i^2} - \sqrt{k^2 - i^2}}{2k + 1}$$

where $r_k = \Delta k$, $y = \Delta i$ and $r_s = \Delta N$ has been used and the indice i takes on the following values: $i = 0, 1, 2, \ldots, N-1$. K is the Gladestone-Dale constant, e.g., for $\rho_\infty K = 2.98 \times 10^{-4}$ for air when $\rho_\infty = 1$ atm.

Because the interferometer comparison scene is recorded in air and the test scene recorded with combustion products, account must be made for different chemical species. The fringe number equation is,

$$S = \frac{1}{\lambda} \int (n - n_\infty) \, dx$$

Using the Gladestone-Dale relationship, $n-1 = \beta \frac{\rho}{\rho_s}$, one gets

$$S = \frac{\beta_\infty}{\lambda} \frac{\rho_\infty}{\rho_{0\infty}} \int \left(\frac{\beta_\tau}{\beta_\infty} \frac{\rho_{\infty 0}}{\rho_{\tau 0}} \frac{\rho}{\rho_\infty} - 1 \right) dx$$

where

S = fringe shift

λ = irradiation wavelength

β = Gladestone-Dale constant

ρ = density

x = distance along light ray

subscripts

∞ = comparison scene conditions of air before burner is ignited

τ = test scene conditions having combustion product species

o = standard conditions at which β's are evaluated

The procedure then is one of calculating the quantity $\frac{\beta_\tau}{\beta_\infty} \frac{\rho_{\infty o}}{\rho_{\tau o}} \frac{\rho}{\rho_\infty}$ by the standard Abel technique just described and then dividing by the quantity $\frac{\beta_\tau}{\beta_\infty} \frac{\rho_{\infty o}}{\rho_{\tau o}}$ to get the density ratio, $\frac{\rho}{\rho_\infty}$, which is the flame density normalized by the density of air at the conditions of the comparison scene recording (room temperature and pressure).

The value of β_τ is calculated as follows from the Gladestone-Dale equation for species $i = 1, 2 \ldots N$. For any dilute gas,

$$n - 1 = \Sigma \beta_i \frac{\rho_i}{\rho_{oi}}$$

$$= \rho \Sigma \frac{\beta_i}{\rho_{oi}} C_i$$

where β_i is evaluated for species i and C_i is the mass fraction. However, by definition

$$n - 1 = \beta_\tau \frac{\rho}{\rho_{o\tau}}$$

Therefore, combining these two equations yields

$$\beta_\tau = \rho_{o\tau} \Sigma \frac{C_i \beta_i}{\rho_{oi}}$$

ρ_{oi} can be shown to be 0.00279 m_i lb_m/ft^3 at atmospheric pressure and 0°C where m_i is the molecular weight of species i.

As an example, consider the case of burning butane whose chemical reaction at stoichiometric conditions is

$$CH_3 (CH_2)_2 CH_3 + 6.5O_2 + 6.5 (3.76) N_2 \longrightarrow$$
$$4 CO_2 + 6.5 (3.76) N_2 + 5 H_2O$$

From this reaction the following is calculated:

Reaction Products	C_i	β_i	ρ_{oi}	$\beta_i \rho_{oi}$	$C_i \rho_{oi}$	m_i	$C_i \beta_i \rho_{oi}$
CO_2	0.186	4.51×10^{-4}	0.1275	3.53×10^{-3}	0.0237	44	0.656×10^{-3}
N_2	0.723	2.97×10^{-4}	0.0812	3.66×10^{-3}	0.0587	28	0.265×10^{-3}
H_2O	0.095	2.54×10^{-4}	0.0522	4.88×10^{-3}	0.00496	18	0.464×10^{-3}

$$\rho_o = \Sigma C_i \rho_{oi} = 0.0874$$
$$\Sigma C_i (\beta_i/\rho_{oi}) = 3.770 \times 10^{-3}$$

Therefore,

$$\beta_\tau = (0.0874)\ (3.77 \times 10^{-3})$$
$$= 3.29 \times 10^{-4} \quad \text{(NOTE: for air } \beta_\infty = 2.92 \times 10^{-4})$$

The average molecular weight is calculated as,

$$\frac{1}{\bar{m}} = \Sigma \frac{C_i}{m_i}$$

After some algebra

$$\bar{m} = 28.3 \text{ (for air } \bar{m} = 28.7)$$

From these results, one can show that $\frac{\beta_\tau}{\beta_\infty} \frac{\rho_{\infty o}}{\rho_{\tau o}} = 1.14$.

5. RESULTS

5.1 SEQUENCE OF PROGRESS AND PROBLEMS SOLVED

Before proceeding with a discussion of the results, a chronological perspective of the progress and problems leading to those results will be given. The following areas were investigated and progress made as indicated.

- Film fogging problem solved with filters and shutters
- Laser light absorption shown not to be a problem
- Holograms of the fuel spray and holographic interferograms of the flame were recorded with 17 inch scene depth holocamera
- Holographic interferograms were recorded of the flame with a 41 inch scene depth holocamera
- Finite fringe interferograms were recorded of flame
- Both infinite fringe and finite fringe interferograms were recorded of a small propane burner and of a hot air source
- Preliminary data reduction of the interferograms was accomplished
- Preliminary thermocouple temperature measurements were made of the burner flame.

5.2 HOLOGRAMS

A hologram* of a 1 inch square grid coordinate system placed in the scene at 45° to the beam axis is shown in Figure 8. A faintly observed 1 cm square grid located at the objective lens is also shown. The copy camera was focused on the coordinate system in the foreground and thus the grid in the background is out-of-focus.

The purpose of recording holograms, as distinguished from holographic interferograms, on this program was to observe the fuel spray. The effort was meant to be on a quick look basis rather than an in depth study.

---

* These figures are called holograms and interferograms although they are more properly identified as photographs of one view of the reconstructed holographic scene, whether a hologram or holographic interferogram.

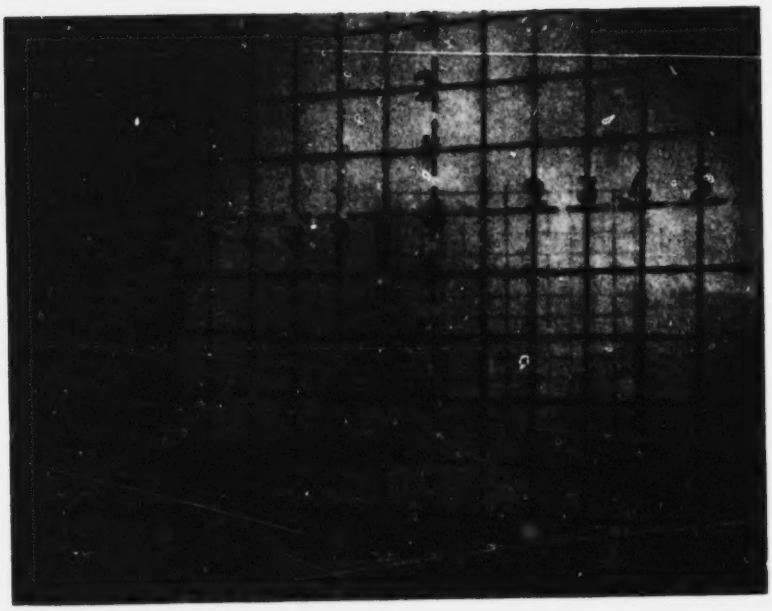

Figure 8. Hologram of coordinate systems and background grid.

In Figure 9 is shown a burner spray pattern on the windows of the burner box. The burner was off but the spray was allowed to run for 2 seconds before the hologram was recorded. Without burning, the spray quickly mars the transmission through the box as can be seen from the irregular visibility of the background centimeter grid. The wavelike pattern on the walls is reproducible qualitatively from shot to shot. Agglomerated droplets are visible on the windows besides the large wave-line films observed.

In Figure 10 is shown a burner spray pattern which was recorded by placing an opaque checkerboard grid at the plane of the centimeter grid (i.e., at the objective lens). The burner box windows were removed for this test. Recording the spray hologram in this way allows dark field illumination viewing of the spray pattern against the opaque strips of the checkerboard. There was no preponderance of evidence that spray droplets could be resolved in this hologram with the unaided eye, although individual scattering centers (droplets) were observed on some of the other holograms near the periphery of the lens. The droplet size is believed to be ~25 microns.* The single droplets could be recorded via low angle forward scattering holography using a two- or three-beam holocamera arrangement as demonstrated and described in References 13 and 14.

These holograms were recorded in the small holocamera because resolution of individual droplets is expected to drop off as scene depth is increased. No further work or analysis was done on either the spray holograms or on optimizing the resolution of the holocamera in this "quick-look" effort.

5.3 HOLOGRAPHIC INTERFEROGRAMS

Short Scene Holocamera Results

A two inch diameter, leaf-type mechanical shutter was located and installed before the film plate holder of the holocamera apparatus. The shutter speed was measured photoelectrically and determined to be 6 msec; approximately 10 times faster than the focal plane shutter used originally. The faster shutter together with a Wratten No. 70 filter resulted in a successful holographic interferograms of open flame combustion from the ABC MITE Model S oil burner. The recording was free of any objectionable fog.

---

* The resolution of this diffuse illumination transmission holocamera was previously measured using Air Force 1951 resolving power targets and found to be ~25 at a distance of 12 inches from the holographic plate. This work is described in Reference 8.

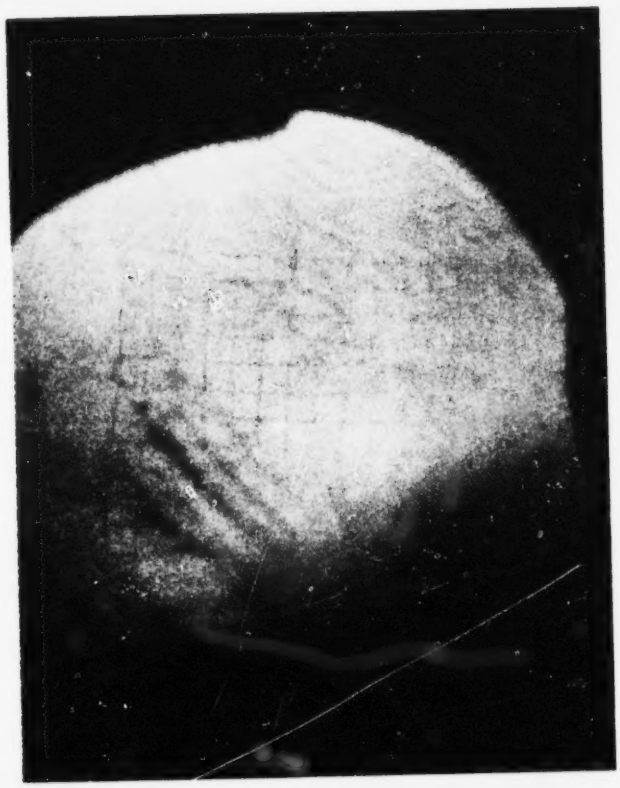

Figure 9.

Burner Spray Pattern Burner Off.
Spray on for 2 seconds.

Reproduced from best available copy.

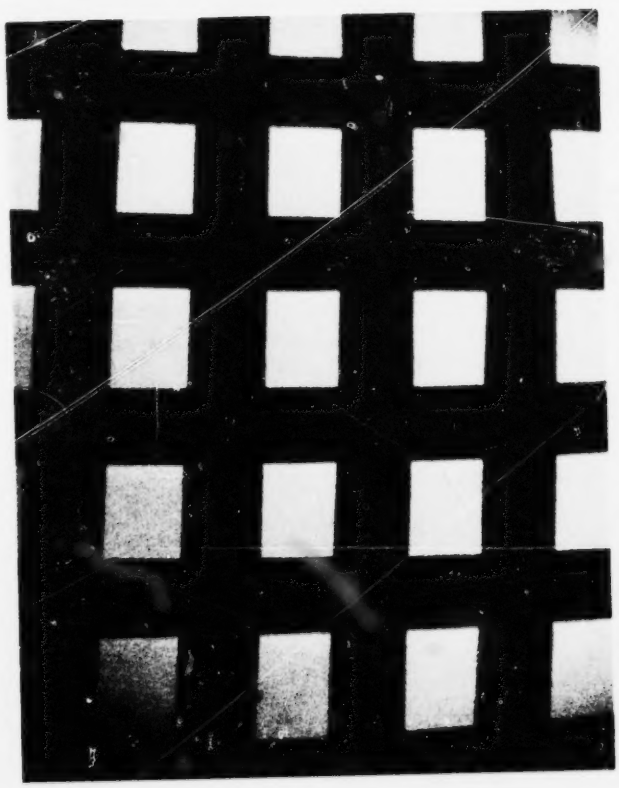

Figure 10.

Burner Spray Pattern Burner Off.
Spray on 2 seconds.

The recording was made on Agfa 8E75, 4 x 5 inch plate; however, since the shutter diameter was only two inches, one had the feeling of looking through a "knothole" when viewing the virtual image reconstruction. This is seen in the accompanying reconstruction photographs (Figure 11). The reconstruction photos were made using a bellows-type view camera with a 127 mm focal length lens at an f/11 aperture. All reconstruction photographs were recorded on Polaroid Type 52 film. In the first photograph, the view camera was focused on a centimeter grid inscribed on the 1/4-inch acrylic sheet covering the quadruple lens set of the holocamera. In the original scene, this grid was located approximately 15 inches from the center of the holographic film plate. The succeeding shots were made by extending the bellows from the rear (film holder) side of the camera in one inch increments. In addition to changing the focus, the reconstructed image was simultaneously magnified.

The purpose of this test was to determine the effect of increased shutter speed on the fog level of the Agfa plate. Since the flame was essentially unconfined, burner operating conditions were not monitored and systematic reconstruction procedures were not used as quantitative data would not be reduced from this interferogram. From a qualitative point of view, the test was very successful in that a fog free interferogram of burner combustion was achieved. The series of four reconstruction photos demonstrate the three dimensionality of the holographic interferogram and show that the combustion scene is not opaque to the ruby scene light.

Careful examination of the four reconstruction photographs of Figure 11 reveal subtle changes in the fringe patterns at different focal positions of the camera. The quantity and pattern of the fringes indicate a high degree of turbulence in the flame. When viewing the reconstruction from extreme angles against a dark field background, it is possible to detect individual oil droplets by scattered laser scene light. This is not seen in the accompanying reconstruction photographs. The droplets may be too small to resolve in the diffuse scene light. This observation does suggest, however, that forward scattered light holography techniques could be employed to assess droplet life and number density distribution in the combustion volume.

A larger 3.5 inch diameter shutter, mentioned in Section 2.2, was installed and used successfully to record holographic interferograms of the burner flame. This shutter has three times the area of the former shutter and hence represents an improvement in holographic coverage of the flame. The speeds of the mechanical leaf-type shutter are 9, 18, and 40 milliseconds. To date only the 9 millisecond exposure has been used. The Wratten No. 70 filter was also used.

Reproduced from
best available copy.

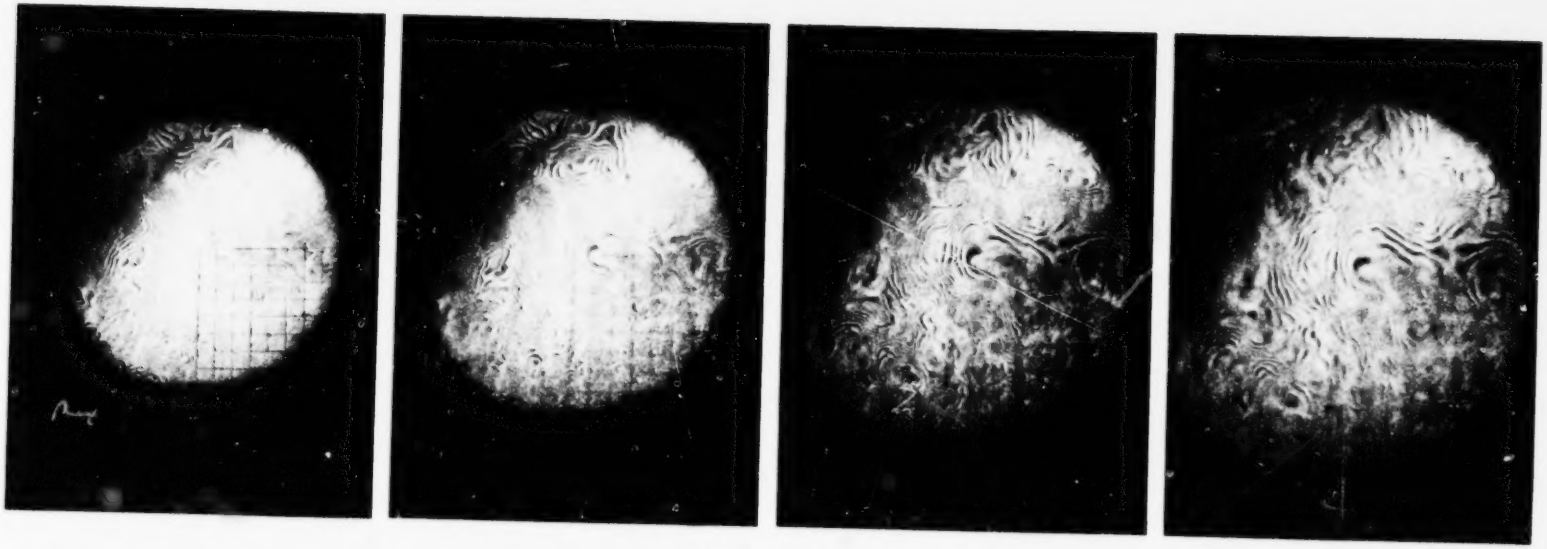

Figure 11. Reconstruction photographs of a ruby laser interferogram of open flame combustion from the ABC Mite oil burner. The photos differ by the focus of the copy camera. The direction of flow is from right to left.

A description of some of the burner infinite fringe holographic interferograms recorded with the short focal length holocamera is given next. Figures 12 and 13 show two reconstructions of the same holographic interferogram. The burner head is just visible in the right side of the picture. A centimeter grid is shown out of focus in the background. The view camera used in reconstruction had a focal length of 127 mm. Figure 12 was copied at f/32 for 6 minutes. Figure 13 was copied at f/32 for 6 seconds. The difference between the two reconstructions is that the plate photographed in Figure 13 had been bleached. This process returns the silver to silver halide and allows a brighter picture to be recorded. The right central portion of the photographs, where the turbulent flame predominates, shows close fringe spacing and large gradients. Outside this central region, cooler gases exist and larger fringe spacing is observed.

The most important feature observed in these two figures is that the burner flame is very turbulent. The eddies appear to range in size by at least a factor of 30.

Shown in Figure 14 is a reconstruction of a burner interferogram in which the burner had been turned off for 1 second. Residual burning lasts for about 2 seconds. The fringe spacing is much larger in Figure 14 than for Figures 12 and 13 indicating that the density gradients are lesser for the former case than the latter two cases. Different regions of the hot gas are observed here just like in the former case. These regions are delineated by changes in the fringe spacing. Observed immediately to the left of the burner head is a small contour fringe. This fringe is believed to be related to evaporation of the spray in this region. In the left hand portion of the picture the oil spray has impinged on the window producing a poorer quality gas interference pattern there.

In Figure 15 an infinite fringe interferogram of the ABC Mite burner flame is shown at a distance of 10 inches from the burner head. Irregular large scale fringes are in the upper left diagonal half of the picture indicating small gradients and low temperatures. Smaller fringes are in the lower half indicating large gradients and high temperatures. It appears that the luminous part of the flame is in the lower half region. Strong turbulence confuses the fringe structure and numbering in that region.

Long Scene Depth Holocamera Results

In order to see the flame boundaries, the holocamera was increased in scene depth from 17 to 41 inches (see Section 2.2). An infinite fringe interferogram of the ABC Mite flame confined by the burner box is shown in Figure 16. The fringes are better resolved at the boundaries, but it is not possible to follow one fringe completely because of the extreme turbulence.

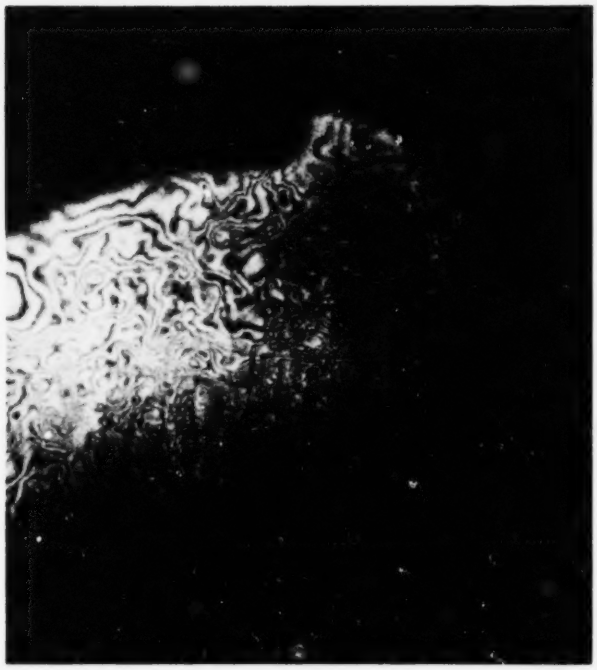

Figure 12. Burner Interferogram. Burner on For 5 Seconds.

Reproduced from best available copy.

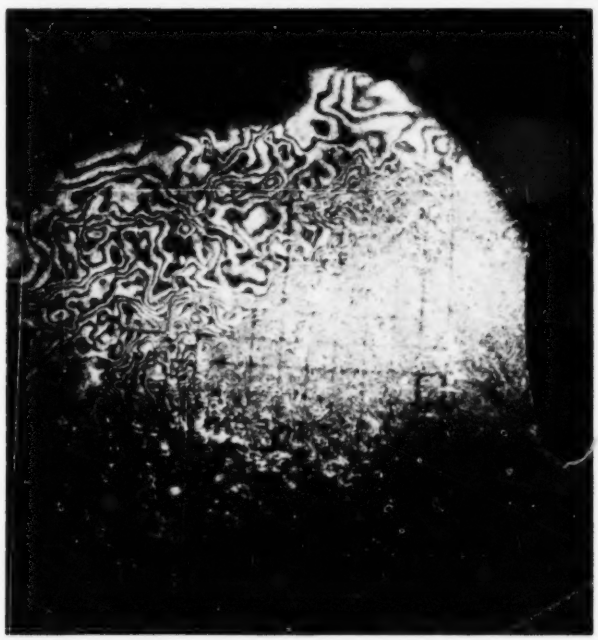

Figure 13. Burner Interferogram. (Reconstructed from Bleached Plate). Burner on for 5 Seconds.

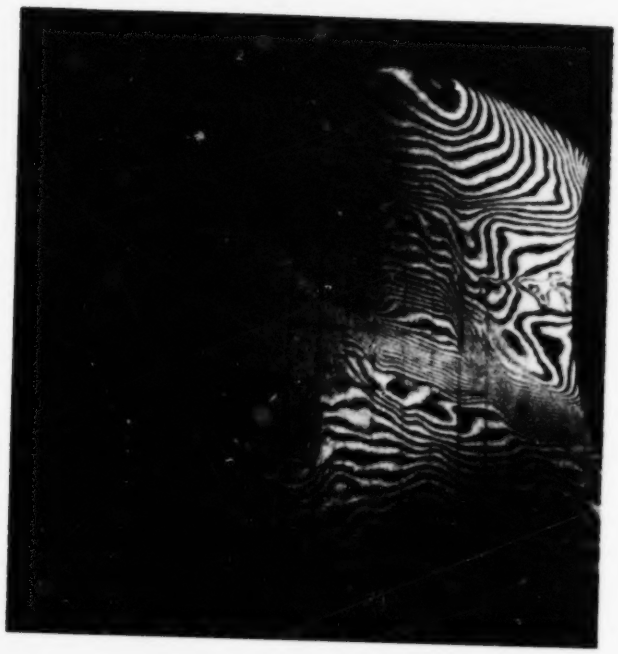

Figure 14. Burner Interferogram (Reconstructed from Bleached Plate). Burner Off For 1 Second.

Reproduced from best available copy.

Figure 15. Infinite Fringe Interferogram of ABC Mite Burner Centered at 10 Inches From Head.

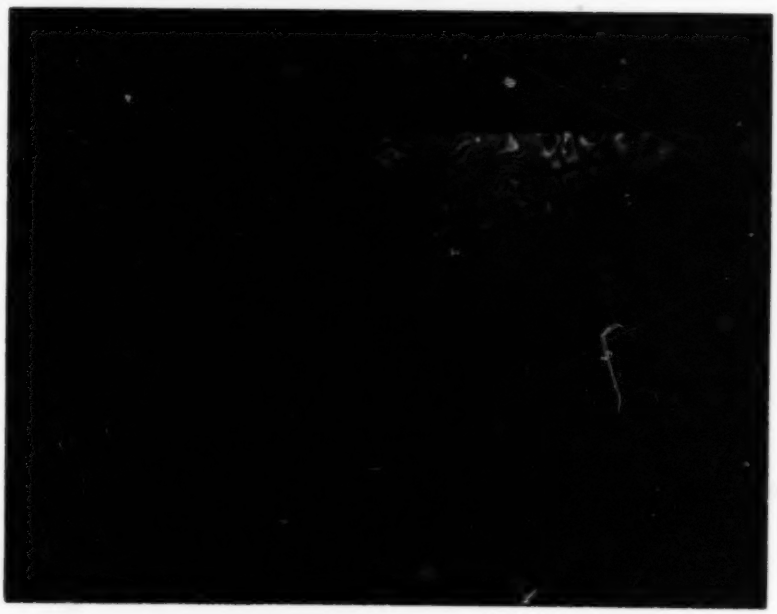

Figure 16. Interferogram of ABC MITE Burner.

Reproduced from best available copy.

During our work with the ABC Mite burner, it was noticed that the starting transient of the burner was not a smooth process. Intermittent, repetitive starts were common. Two interferograms showing this phenomena are given in Figure 17 and 18. In Figure 17 combustion extinguished itself completely after an initial burning cloud of fuel oil ignited. In Figure 18 a second burning cloud appears to be emerging from the burner. It is anticipated that poor combustion and high emissions are present at this time.

A finite fringe interferogram of the ABC Mite after 1/2 second combustion is shown in Figure 19 with one of the thermocouple probes. An early time recording was made to avoid the large thermal free convection currents which initiate subsequently and add to the obscuration of the fringe pattern. The probe was included to show what disturbance, if any, was introduced by the probe. It is believed that the nonsymmetrical fringe pattern is caused by combustion turbulence and not the probe. The fringe resolution is particularly good in this photograph, accentuating the turbulence present in the flame. The flame appears to be asymmetric with respect to the spray axis which is along the burner head centerline. A preliminary interpretation of this fringe pattern suggests that combustion may not have been fully established and that the flame had lifted off the face of the burner. As noted, this recording was made very early after ignition.

Next it was decided to see whether the Beckett and ABC Standard burners were as turbulent as the ABC Mite. An interferogram of the Beckett is shown in Figure 20 at a point 1 second after ignition and presumably past the combustion transient discussed earlier. The characteristic feature of this interferogram contrasted to the ABC Mite is that the flame of the Beckett appears more concentrated along the burner centerline. Possibly this occurs because of poorer spray distribution. It may be a contributing factor to the Beckett emitting twice as much NO as the Mite, a result determined in Reference 1. Some attempts at data analysis were made on this interferogram. This is discussed in Section 5.4.

The reconstruction photograph of Figure 21 is a finite fringe interferogram recorded using the Beckett burner. The recording was made prior to ignition of the oil droplet spray. The fringe shift apparent in this illustration is due to changes in the optical path from vaporizing fuel droplets. The pattern appears symmetrical in the shape of a cone with the exception that some fringe shift appears at the top of the burner head near the face. This suggests that the spray pattern produced by this burner is not always entirely uniform. The recording may have caught the very onset of fuel spray ignition in this one local region.

Figure 17. Infinite Fringe Interferogram Combustion Starting Transient in ABC Mite Showing Intermittent Combustion.

Reproduced from best available copy.

Figure 18. Infinite Fringe Interferogram Combustion Starting Transient in ABC Mite Burner Showing Two Burning Clouds of Gas.

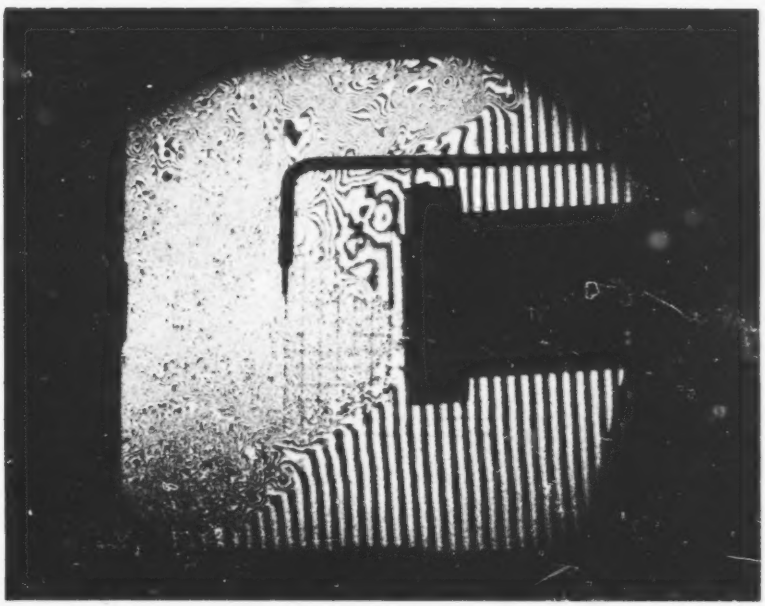

Figure 19. Reconstruction photograph of the Mite burner approximately 1/2 second after ignition. This finite fringe interferogram illustrates the effect of placing a thermocouple probe in the combustion zone.

Reproduced from best available copy.

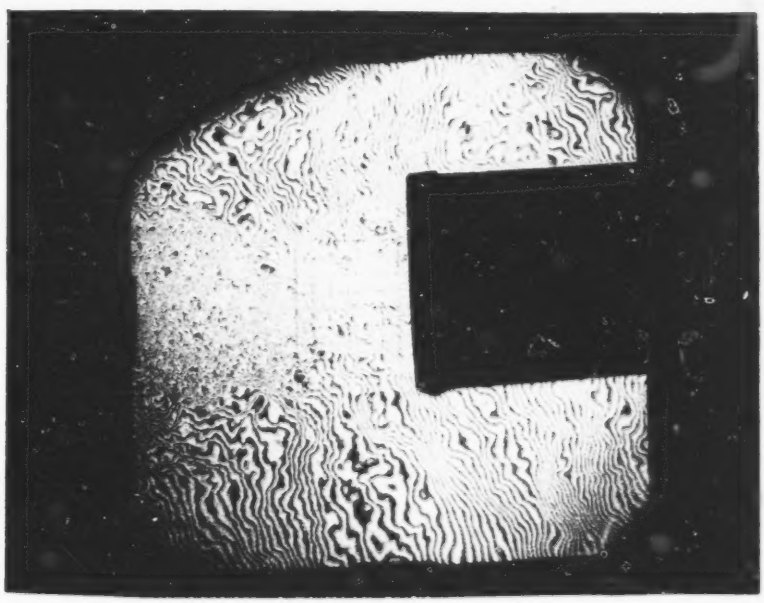

Figure 20. Reconstruction photograph of a finite fringe interferogram of the Beckett oil burner recorded approximately 2 seconds after ignition. Note the significant reduction in the level of turbulence with this burner in comparison with the Mite illustrated in Figure 19.

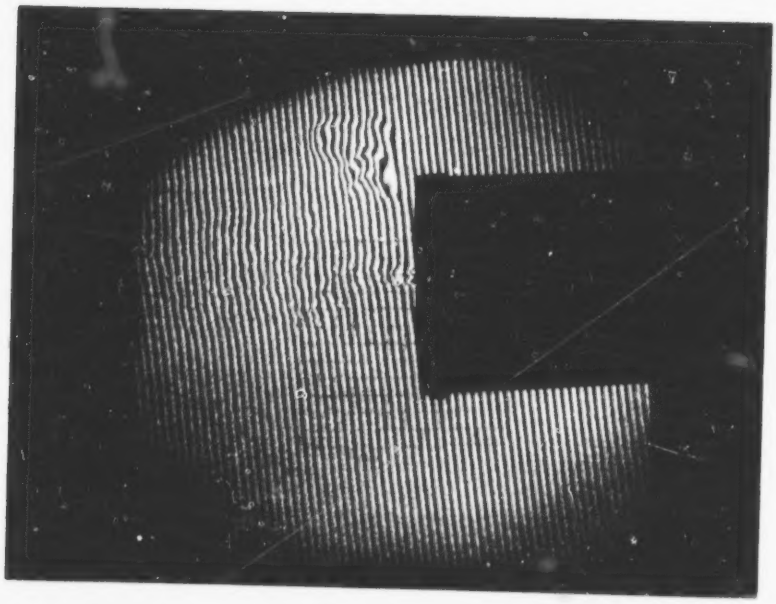

Figure 21. Reconstruction photograph of a finite fringe interferogram of the Beckett oil burner. The recording shows the fringe shift due to vaporizing fuel spray prior to full ignition and combustion. Note the discontinuity at the top of the burner suggesting a non-uniform spray distribution and/or the onset of combustion in this local region.

Because of the large scene filled with a hot, turbulent burner flame, the fringes are irregular, closely spaced and difficult to interpret. It was suggested that the understanding of burner combustion, especially interferometrically, would proceed faster if smaller burners or a small air heater might be studied in a somewhat more controlled manner. To this end, both a Bernzomatic propane flame and a laboratory hot air gun were recorded. These are illustrated in Figures 22, 23, 24, and 25. Both infinite fringe and finite fringe interferograms were recorded. Bouyancy effects are particularly noticeable. As the hot gas forward velocity decreases due to entrainment, bouyancy forces cause the gas to rise. The important features to observe of the small scale burners are the following:

1. Fringe spacing is large enough to resolve individual fringes.
2. Lateral boundaries are wholly contained within the pictures so that fringe numbering can be accomplished.
3. Turbulence is not so intense that the interpretation is obscurred.

An improvement to the study of small burners would be to orient the flame axis vertically so that the bouyancy forces would be symmetrical to the normal symmetries of the flame such as that shown in Figure 26 of the Bernzomatic recorded during an independent TRW study. Data reduction can be best achieved for symmetrical fringe patterns or patterns perturbed only slightly from a mean symmetrical pattern. Large asymmetries can be treated if a wide angle camera is used to record wide angle data. Some data reduced from the Bernzomatic will be discussed in Section 5.4. The hot air gun interferograms shown in Figures 24 and 25 have lesser fringe shifts than the Bernzomatic because of lower temperature. Turbulence is in evidence on a much broader scale range than for the Bernzomatic, which has larger scales represented largely because of the induced motion caused by bouyancy forces. The turbulence in evidence in Figures 24 and 25 was caused by a grid and small blower, part of the air gun. Preliminary data were also reduced for the gun and is given in Section 5.4.

5.4 INTERFEROGRAM DATA REDUCTION

The Abel inversion integral (Section 4) was applied to 3 cases to obtain some preliminary feasibility of reducing the data on the Beckett (Figure 20), the Bernzomatic (Figure 26) and the hot air gun (Figure 24).

Because the fringes could not be resolved near the centerline of the Beckett, data could only be reduced from .5 burner head radii out to the outer boundary as shown in Figure 27. The main feature is the very large temperature gradient starting at about $R/R_B = 0.6$. The gradient there is

$$\frac{\Delta T/T}{\Delta R/R} = 7.5 \quad \text{or} \quad \frac{\Delta T}{\Delta R} = 800°F/\text{inch}.$$

Figure 22. Infinite fringe interferogram of Bernzomatic flame.

Reproduced from best available copy.

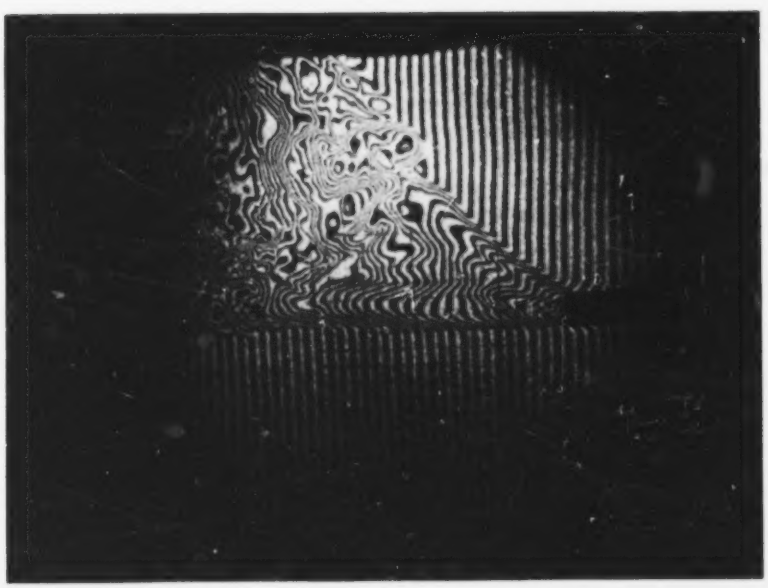

Figure 23. Finite fringe interferogram of Bernzomatic flame.

Reproduced from best available copy.

Figure 24. Infinite fringe interferogram of hot air gun jet.

Figure 25. Finite fringe interferogram of hot air gun jet.

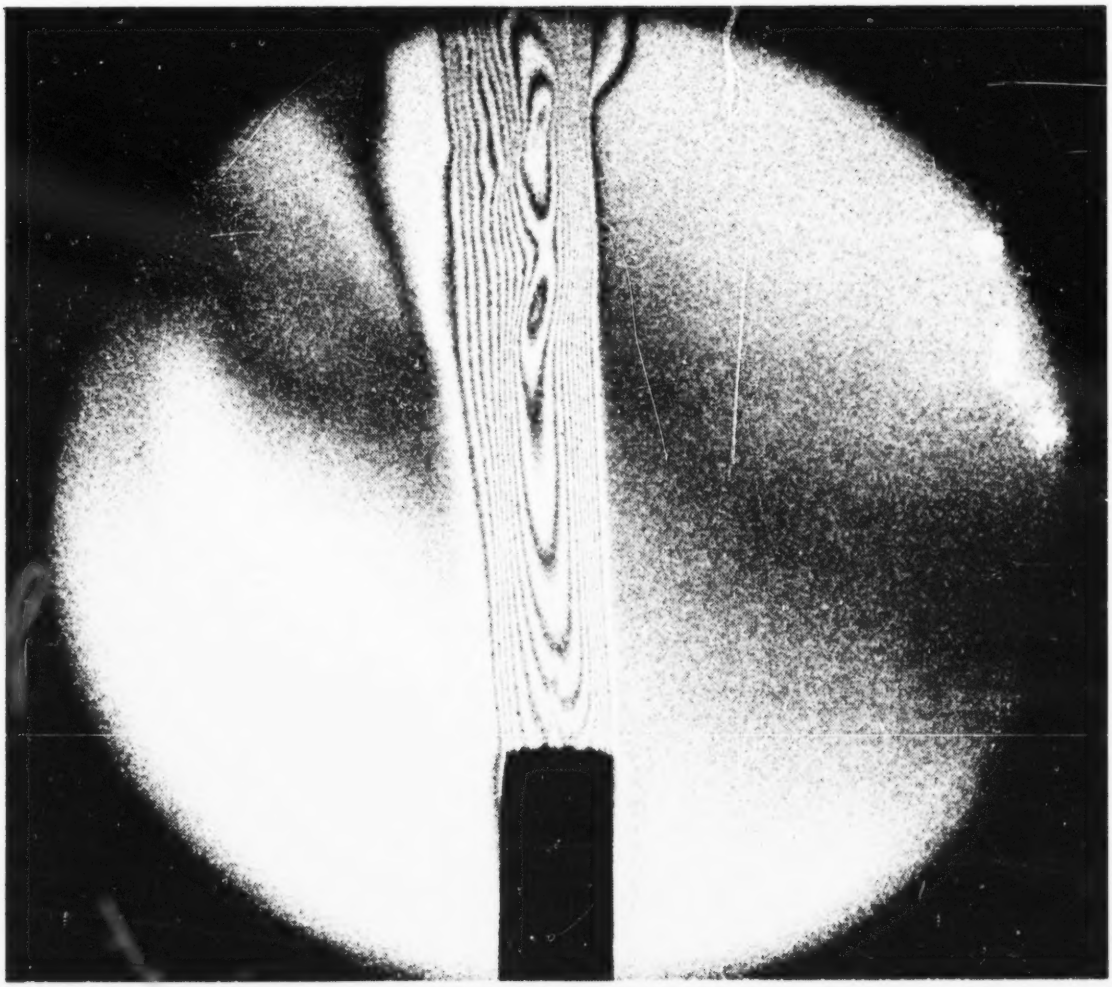

Figure 26. Infinite fringe interferogram of Bernzomatic burner oriented vertically.

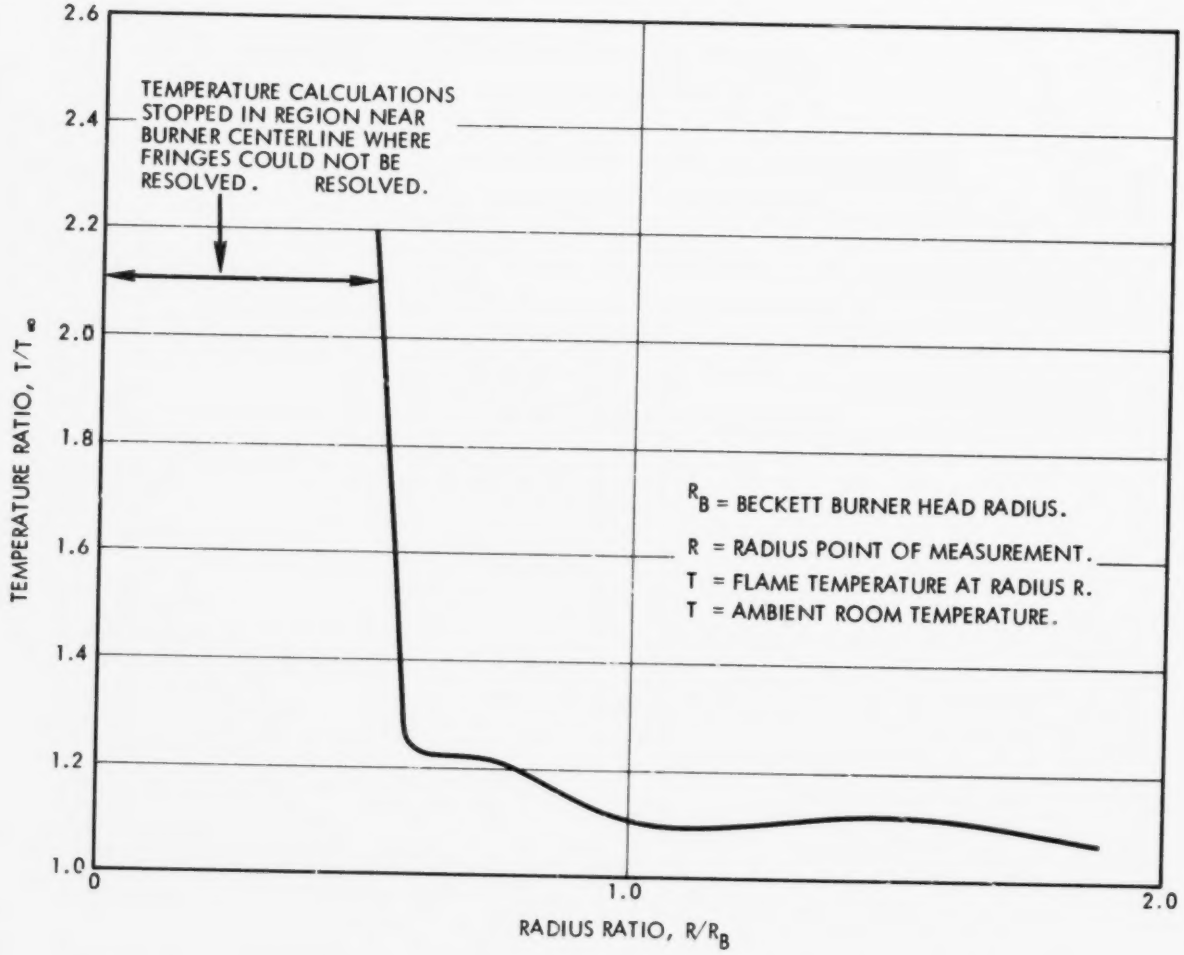

Figure 27. Temperature profile at the exit plane of the Beckett Burner.

A small correction for the fact that the gas in the comparison scene is air and in the test scene is combustion products has not been made but is discussed in Section 4.

The Bernzomatic density profile is shown in Figure 28. The approximation has been made that the indicies of refraction are unchanged between the comparison and test scenes. If account is taken of this effect, as shown in Section 4, the density shown in Figure 28 should be about 15% less. Because the molecular weight is about the same between test and comparison scenes, the temperature ratio is just the inverse of the density ratio. The density drops rapidly at the edge of the burner to a minimum (temperature maximum). This rises to a relative maximum and then to a relative minimum on the centerline. The non-monotonic behavior is believed to be caused by passage of the cool gases into the reaction zone. The temperature gradient at the edge of the Bernzomatic is about a factor of 10 larger than for the Mite. Considerable profile detail can be achieved by this method. Burner turbulence may play a strong role in producing these largely different temperature gradients. For instance, mixing at one edge of a turbulent flame is far more rapid than for a laminar one. This tends to make a more uniform density/temperature jet like that shown for the hot air gun in Figure 29. The temperature of the jet on the centerline is about 100°F above ambient temperature. This result comes directly from the density profile shown and the perfect gas law.

Use of small burners holds greater promise for holographic data reduction in a controlled experiment for the following two reasons:

1. Flame size is smaller, producing fewer fringes which can be resolved and interpreted, and;
2. Flame turbulence level can be controlled by using screens, boundary layer trips, and other forms of turbulence control and generation.

5.5 THERMOCOUPLE MEASUREMENTS

Of the three thermocouple designs fabricated, shown in Figure 7, and discussed in Section 2.3, data have been obtained only with the feasibility model, a 0.051 inch diameter barewire chromel-alumel probe (Figure 7a). The data for the Mite in the burner box are shown in Figure 30. Temperature, 5 inches from the burner head, is shown as a function of radial distance which has been normalized by burner head radius. With a few exceptions, the temperatures are within 100°F for all air mix settings of the Mite. Using a radiation correction established in Section 2.3, the peak temperature should be about 2600°R. Based upon d = 0.051", ℓ = 0.75",

$$H_g = \frac{BTU}{ft^2\ hr°F}, \quad k = 1.12\ \frac{BTU}{hr\ ft°F}$$

(chromel), the conduction error was shown to be negligible. The peak temperature seems low. Possibly, fuel spray is impinging on the thermocouple. More work needs to be done on this type of measurement in the vicinity of the fuel spray.

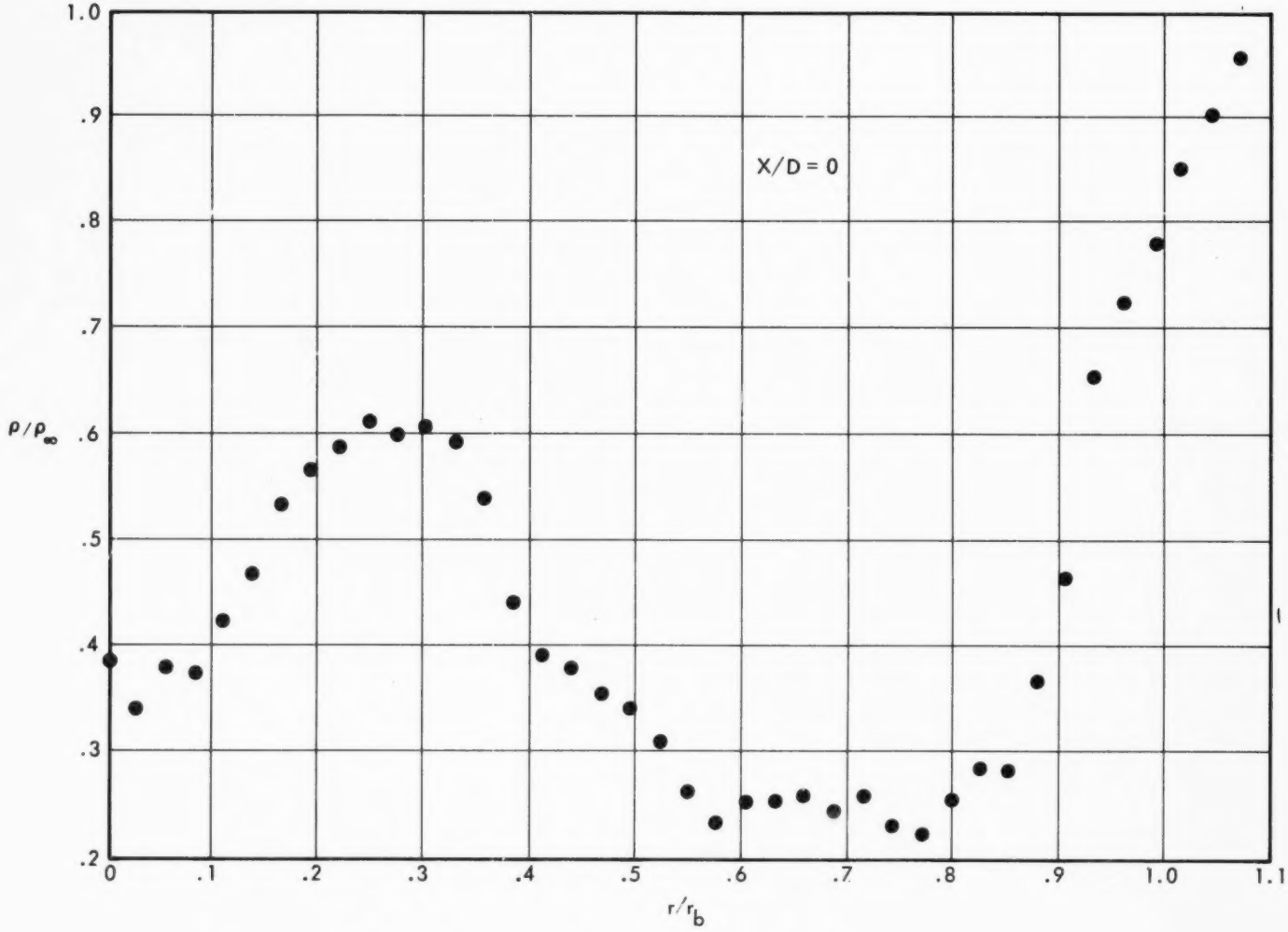

Figure 28. Density profile for Bernzomatic burner at exit plane.

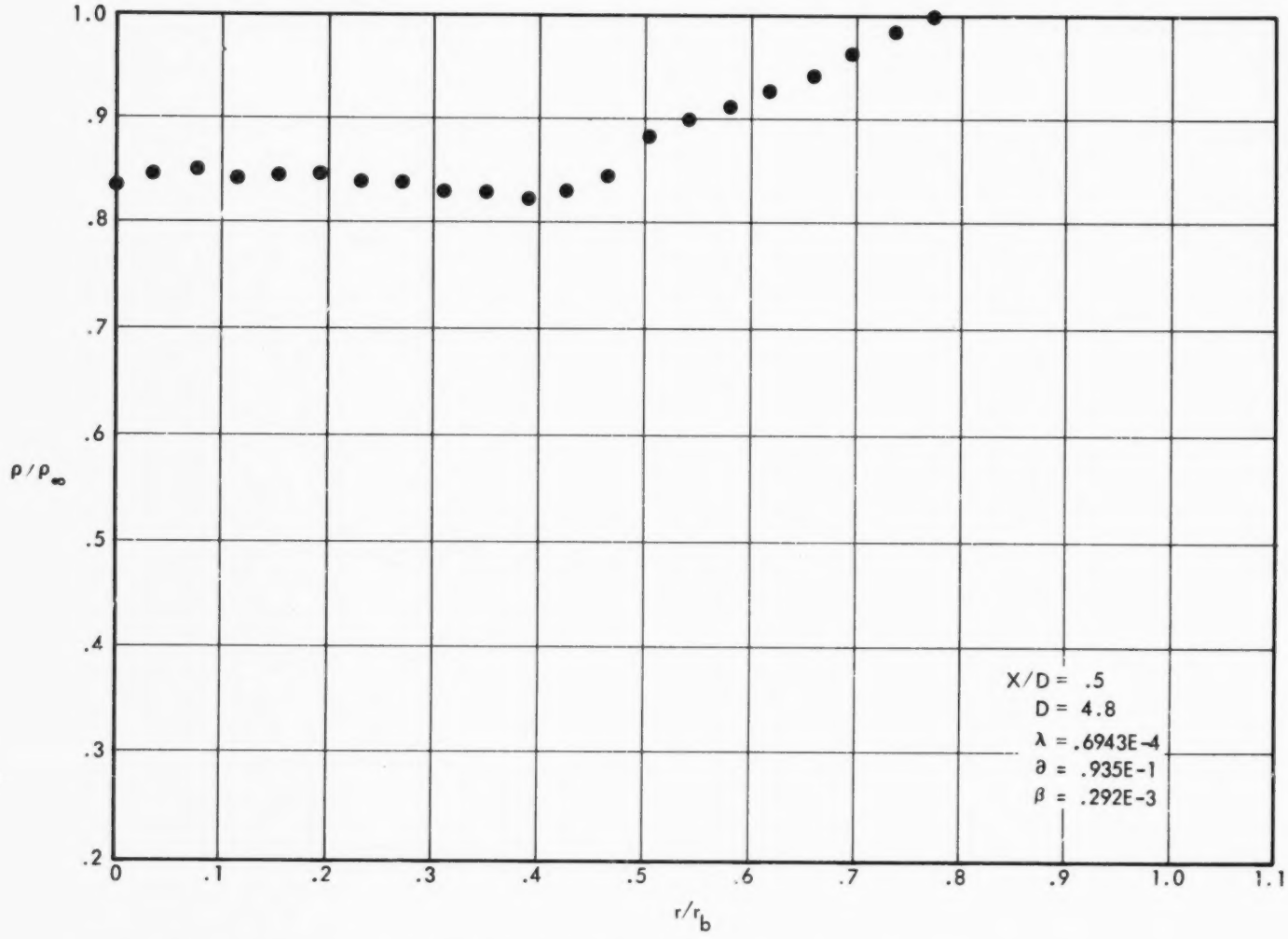

Figure 29. Density profile for hot air gun at Plane 0.5 head diameters from exit plane.

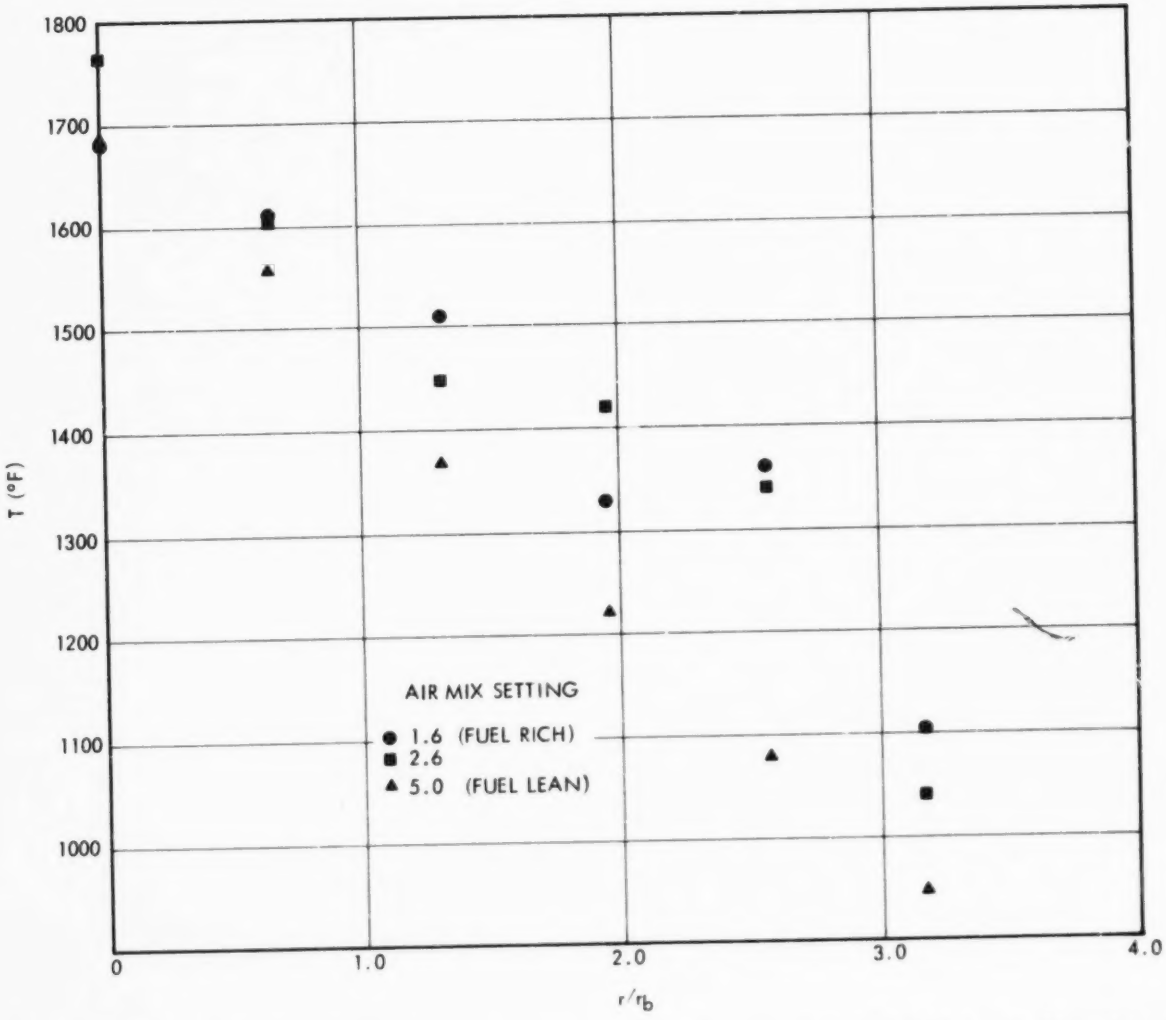

Figure 30. Temperature measurement of the Mite Burner flame using a 0.051 inch diameter barewire chromel-alumel thermocouple.

6. CONCLUSIONS

1. The feasibility of recording fog-free holographic interferagrams of residential fuel fired oil burner flames was demonstrated with two holocameras designed to observe the near and far field of the burner.

2. The most important feature observed interferometrically was that the flame structure is extremely turbulent. This turbulence made it impossible to resolve the fringe pattern on the centerline of the burner.

3. Preliminary data reduction of the interferograms showed that on the outside edge of the burner, the temperature gradient, $\frac{\Delta T}{\Delta R}$, was about 800°F/inch.

4. Barewire thermocouple measurements made of the flame were corrected for radiation, and are believed to be lower than the true flame temperature because of fuel droplet impingement and evaporation.

5. Excellent quality holographic interferograms were recorded of a small burner (Bernzomatic burner). Fringes could be resolved, read and interpreted. Temperature gradients calculated at the edge of this laminar flame were about a factor of 10 higher than for the Beckett fuel oil burner turbulent flame supplied by EPA.

6. Recording a holographic interferogram of a hot air gun showed the feasibility of controlling the turbulence level of a flame-like hot gas. Preliminary data were also reduced in this case.

7. RECOMMENDATIONS

1. Study the full-scale burner using holographic interferometry by sampling only a small part of the burner flame. This concept can be implemented by using a "cookie cutter" manifolded laterally and vented apart from the test section.

2. Study a subscale burner which produces a resolvable number of fringes, provides more flexibility and control of the pertinent variables, especially the mixing and turbulence factors. Measure mean flow and turbulence properties of the flame.

3. Study both burners cited in (1) and (2) above using cooled probe anemometry. Fast response .006 inch diameter cooled quartz tube probes (with platinum film sensing element) are available commercially and would provide such measurements as turbulence intensity, power spectral density, auto correlation and eddy integral scale. Ion probes may also be considered for this task. The thermocouple probes designed and fabricated under the present contract should be tested and evaluated. These measurements are necessary to supplement and validate the interferometry measurements of mean and fluctuating properties. Temperature measurements in the presence of liquid droplets may require design of a special temperature/enthalpy probe.

4. Study combustion of liquid droplets holographically to determine a model for liquid droplet combustion in a turbulent flow field. Determine the relationship between droplet size and turbulent eddy size for most efficient combustion.

8. REFERENCES

1. Howekamp, D. P., "Flame Retention - Effects on Air Pollution", Paper submitted at the Ninth Annual Convention, National Oil Fuel Institute, Atlantic City, N.J. 9-11 June 1971.

2. Matthews, B.J., and Wuerker, R.F., "The Investigation of Liquid Rocket Combustion Using Pulsed Laser Holography", AIAA 5th Propulsion Joint Specialist Conference, United States Air Force Academy, Colorado, Springs, Colo., 9-13 June 1969.

3. "Studies of the Erosion of Aluminum Cartridge Cases", TRW Report No. 13774-6002-RO-00 Army Contract DAAA25-70-C-0152, Oct. 1970.

4. Witte, A.B., Fox, J., and Rungalaier, H., "Localized Measurements of Wake Density Fluctuations Using Pulsed Laser Holographic Interferometry," Presented at AIAA Reacting Turbulent Flows Conference, San Diego, Calif., 17-18 June 1970.

5. Witte, A.B., Fox, J., and Rungaldier, H., "Holographic Interferometry Measurements of Mean and Localized Fluctuating Wake Density Field for Cones Fired at Mach 6 in a Ballistic Range", AIAA Paper 71-564 Presented at AIAA 4th Fluid & Plasma Dynamics Conference, Palo Alto, Calif., 21-23 June 1971.

6. Witte, A.B., Wuerker, R.F., and Heflinger, L.O., "Wide Angle Holographic Interferometry and Data Reduction to Three Dimensional Density Field", Technical Brief, TRW Systems, June 1970.

7. Matthews, B. J. and Kemp, R. F., "Holographic Determination of Injected Limestone Distribution in Unit 10 of the Shawnee Power Plant," TRW Final Report No. 14103-6001-RO-00, EPA Contract CPA 70-4, June 1970.

8. Matthews, B.J., Wuerker, R.F., and Harrje, D.T., "Small Droplet Measuring Technique," Final Report, AFRPL-TR-156, Air Force Rocket Propulsion Laboratory, Edwards, California, July 1968.

9. Witte, A.B., "Three Dimensional Flow Field Analysis by Holographic Interferometry," Final Tech. Rept. 15 Feb. 1971, TRW Report No. 12414-6005-RO-00.

10. Personal communication from W. Kuyhendal to Birch Matthews and Ralph Wuerker, TRW Systems Group.

11. Caldwell, F.R., "Thermocouple Materials", NBS Monograph No. 40 1 March 1962.

12. Weyl, F.J., "Analytical Methods in Optical Examination of Supersonic Flow", Navord Report 211-45, Navy Department Bureau of Ordnance, Washington, D.C., 11 December 1945.

APPENDIX A

Thermocouple Radiation Correction

A simple estimate of the thermocouple radiation error was calculated by assuming that an energy balance exists between the convection heat flux to the wire and the radiation flux away from the wire, neglecting the background radiation back to the wire. The model develops as one considers a section of wire:

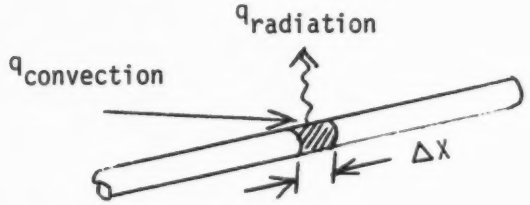

In the steady state, $q_{convection} = q_{gradiation}$ and,

$$h_g (T_g - T_w) = \varepsilon \sigma T_w^4$$

Where re-radiation back to the thermocouple has been neglected so as to yield a conservative estimate.

$$\left(1 - \frac{T_w}{T_g}\right) = \frac{\varepsilon\sigma T_w^4}{h_g T_g}$$

and

$$\frac{T_w}{T_g} = \left[1 + \frac{\varepsilon\sigma T_w^3}{h_g}\right]^{-1}$$

where

T = temperature

h = connective heat transfer coefficient

g = gas side

w = wall

ε = wire emissivity

σ = Stefan-Boltzman constant

For oxidized chromel-alumel thermocouples $\varepsilon \simeq 0.87$.[11] For a 0.011 inch diameter wire at 2200°R and h_g = 72 BTU/ft^2 hr°F, the correction becomes

$$\frac{T_w}{T_g} = 0.84$$

Thus, the gas temperature would be 2600°R. Because the precise value of ε is unknown and may vary as conditions change between stoichiometric and excess air operating conditions, it will be necessary to use a radiation-shielded aspirating thermocouple probe of the type discussed in Section 2.3.

Thermocouple Conduction Losses to Support

The support losses are computed by equating the conductive flux in the wire to the convective and radiative flux from the gas in the steady state:

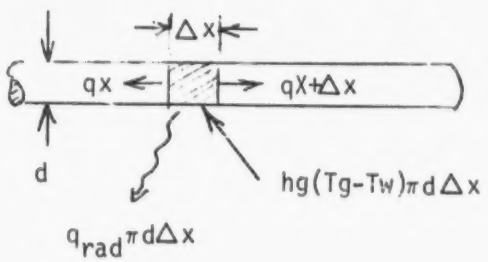

The energy balance in steady state is,

$$(q_{x+\Delta x} - q_x)\,\frac{\pi d^2}{4} - h_g(T_g - T_w)\,\pi d\,\Delta x + q_r\,\pi d\,\Delta x = 0$$

Taking the limit as $\Delta x \to 0$ the differential equiation becomes:

$$\frac{d^2T_w}{dx^2} + 4\,\frac{h_g}{kd}\,(T_g - T_w) - \frac{4qr}{kd} = 0$$

Neglecting radiation and letting $\theta = \frac{T_g - T_w}{T_g - T_{wo}}$, $\bar{x} = \frac{x}{\ell}$, one obtains,

$$\frac{d^2\theta}{d\bar{x}^2} - \kappa\theta = 0$$

The boundary conditions are:

at $\bar{x} = 0$,	$\frac{d\theta}{dx} = 0$	(corresponds to the thermocouple junction location)
$\bar{x} = 0$,	$\theta = 1$	(corresponds to the support location)

The solution is:

$$\frac{T_g - T_w}{T_g - T_{wo}} = \frac{\cosh \kappa\bar{x}}{\cosh \kappa} \xrightarrow[\kappa >> 1]{} 2e^{-\kappa}.\ \cosh \kappa\bar{x}$$

$$= 2e^{-\kappa} \text{ at } \bar{x} = 0 \quad \text{(the junction of the thermocouple)}$$

where

T_g = gas temperature

T_w = wire temperature

$\kappa = \frac{4\,h_g\,d}{\kappa}\left(\frac{\ell}{d}\right)^2$

$\bar{x}$ = x/ℓ normalized distance from junction

h = gas side heat transfer coefficient

d = wire diameter

ℓ = wire length

k = wire thermal conductivity

Subscripts

g = gas

w = wire

0 = supports

For the conditions of these measurements with the .011 inch diameter wire, $\kappa = 38$, the wire junction temperature reads the gas temperature.

Thermocouple Frequency Response

The following discussion is an analysis of the frequency response of a thermocouple wire to the turbulence of a flame. For this analysis, a physical model was assumed where: (1) the thermocouple wire alternately heats and cools via convection; (2) the radiation losses are neglected; and (3) the wire end losses are neglected. In the analysis to follow, the nomenclature listed below is used.

Physical Model:

- wire alternately heats and cools via convection
- neglect radiation
- neglect end losses

d = wire diameter

ρ = wire density

A = wire cross sectional area

T = wire temperature

t = time

c_v = specific heat at constant volume

h = gas side heat transfer coefficient

w = frequency of fluxuation, rad/sec

f = $\omega/2\pi$ (Hertz)

k = thermal conductivity

$Nu = \frac{hd}{k}$ Nusselt number

j = imaginary number

$\alpha = \frac{k}{\rho c_v}$ thermal diffusivity

Subscripts

g = gas

0 = amplitude

w = wire

The energy balance becomes

$$\rho A \, cv \, \frac{dT_w}{dt} = h \, (T_g - T_w) \, \pi d$$

$$\frac{dT_w}{dt} = \underbrace{\frac{hd}{k}}_{Nu} \cdot \underbrace{\frac{k}{\rho c_v}}_{\alpha} \frac{4}{d^2} (T_g - T_w)$$

To solve, one assumes a sinusoidal variation in gas temperature; Let

$$T_g = T_{go} \, e^{-j\omega t}$$

$$T_w = T_{wo} \, e^{-j\omega t}$$

$$\beta = Nu \, \alpha \, \frac{4}{d^2}$$

Then

$$-T_{wo}\, j\omega = \beta\, T_{go} - \beta\, T_{wo}$$

$$\frac{T_{wo}}{T_{go}}\left(1 - \frac{j\omega}{\beta}\right) = 1$$

$$\frac{T_{wo}}{T_{go}} = \frac{1 + j\omega/\beta}{1 + \left(\frac{\omega}{\beta}\right)^2}$$

To get the magnitude of $\frac{T_{wo}}{T_{go}}$, $\left|\frac{T_{wo}}{T_{go}}\right|$,

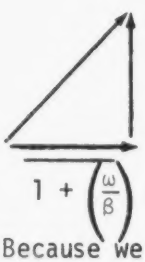

$$\frac{\omega/\beta}{1 + \left(\frac{\omega}{\beta}\right)^2},$$

$$\left|\frac{T_{wo}}{T_{go}}\right| = \frac{1}{\sqrt{1 + \left(\frac{\omega}{\beta}\right)^2}}$$

Because we desire that

$$\frac{T_{wo}}{T_{go}} \rightarrow 1 \qquad \text{this implies that} \qquad \left(\frac{\omega}{\beta}\right)^2 \ll 1$$

Therefore,

$$\frac{T_{wo}}{T_{go}} = 1 - \frac{1}{2}\left(\frac{\omega}{\beta}\right)^2 + \ldots.$$

$$= 1 - \varepsilon$$

where $\varepsilon \ll 1$

Then $\frac{\omega}{\beta} = \sqrt{2\varepsilon} < 1$

and $$f = \frac{4\, Nu\, \alpha \sqrt{2\varepsilon}}{2\pi d^2}$$

For the conditions encountered here

$d = 0.11$,

$Nu = 1.5$ based on Reynolds number of 5

$\alpha = \frac{0.24\ ft^2}{hr}$,

and specifying that

$$1 > \frac{T_{wo}}{T_{go}} \geq .9,$$

the frequency thatone can measure becomes

$$f \leq 34\ Hz$$

This f corresponds to our being able to measure an eddy size A, of

$$\Lambda = \frac{u}{f} = \frac{1\ ft/sec}{34\ Hz} = .029\ ft\ (.348\ in)$$

where u is the convection velocity. Observation of the existing flame interferograms show that the predominant eddy size is this size or larger so that recording should be possible.